Glacial-interglacial variations in sediment organic carbon accumulation and benthic foraminiferal assemblages on the Bermuda Rise (ODP Site 1063) during MIS 13 to 10

Maria Serena Poli,[1] Philip A. Meyers,[2] Robert C. Thunell,[3] and Marco Capodivacca[1,4]

[1]   We have determined organic carbon concentrations and isotopic compositions and benthic foraminiferal assemblages in sediments deposited between ∼500 and 340 ka at ODP Site 1063 on the northeastern flank of the Bermuda Rise. This time interval includes Marine Isotope Stage (MIS) 11, a particularly warm and long interglacial that was similar to today, and MIS 12, one of the most severe glacials of the last 600 kyr. During MIS 11.3, the peak of interglacial warming, organic carbon accumulation rates are low and benthic foraminiferal assemblages are dominated by *Nuttallides umbonifera*, a species indicative of oligotrophic environments. Higher accumulation rates during MIS 12 and 10 correspond with elevated sedimentation rates (33–36 cm/kyr). This pattern implies a combination of enhanced delivery and improved preservation of sediment organic matter during these glacial times. Organic δ^{13}C values are less negative during MIS 12 and MIS 10 than during MIS 11, which is consistent with greater glacial-stage marine productivity. High relative abundances of *Oridorsalis umbonatus* during glacial intervals probably records a low but sustained flux of highly degraded organic material. Large, recurrent fluctuations in the abundance of *Epistominella exigua* at the beginnings of the MIS 12 and MIS 10 glaciations suggest a marked increase in local phytoplankton blooms at these times and consequent delivery of phytodetritus to the seafloor. The most likely causes of these variations are changes in the position and strength of the Gulf Stream and its associated cold-ring eddies, combined with increased advection of terrigenous sediments from northerly locations during glacial lowstands.

1.   Introduction

[2] Marine primary productivity is an important component of the global carbon cycle, where photosynthesis removes carbon dioxide from surface waters, and sinking organic matter transfers carbon to deep waters and marine sediments in a process known as the "biological pump" [*Broecker*, 1982; *Shackleton et al.*, 1983; *Mix*, 1989]. Primary productivity at the ocean surface regulates the concentration of CO_2 in the upper ocean and in the atmosphere [e.g., *Field et al.*, 1998]; for example, without phytoplankton

atmospheric CO_2 concentrations would be close to double present levels [*Sarmiento et al.*, 1990].

[3] The main factors limiting primary productivity are the availability of light and nutrients. Consequently the highest rates of primary productivity are found on continental shelves, sustained by the inputs of nutrients from continental runoff, and in upwelling regions, where cold, nutrient-rich sub-thermocline water is brought to the surface [*Antoine et al.*, 1996, and references therein]. By contrast, the lowest rates are recorded in the subtropical gyres, where strong water column stratification and weak vertical mixing result in significant nutrient depletion of surface waters. At mid and high latitudes, primary productivity is seasonal with maxima in spring and summer, when days are longer, sea ice cover is reduced, and nutrient levels in surface waters are higher due to mixing.

[4] A growing concern is that continued global warming will increase thermal stratification in the open ocean and thus expand the subtropical gyres [*Sarmiento et al.*, 1998; *McClain et al.*, 2004; *Polovina et al.*, 2008]. Indeed, a number of models project a decrease in global mean primary productivity in the 21st century due to a reduction in the Atlantic meridional overturning circulation (AMOC),

[1]Department of Geography and Geology, Eastern Michigan University, Ypsilanti, Michigan, USA.
[2]Department of Earth and Environmental Sciences, University of Michigan, Ann Arbor, Michigan, USA.
[3]Department of Earth and Ocean Sciences, University of South Carolina, Columbia, South Carolina, USA.
[4]Now at TetraTech Geo, Ann Arbor, Michigan, USA.

Corresponding author: M. S. Poli, Department of Geography and Geology, Eastern Michigan University, 250 Strong Hall, Ypsilanti, MI 48197, USA. (mpoli@emich.edu)

enhanced stratification of the water column, and a shallower mixed-layer [e.g., *Schmittner*, 2005; *Steinacher et al.*, 2010]. However, other models predict an increase in global primary productivity [*Sarmiento et al.*, 2004; *Schmittner et al.*, 2008] driven by warmer temperatures and consequent enhancement of phytoplankton growth rates.

[5] Investigations of past changes in primary productivity, especially during intervals of extreme climate conditions, can provide useful insights on how marine productivity is affected by changes in climate and ocean circulation. Data from the midlatitude North Atlantic (north of 45°N) indicate that during the last glacial maximum (LGM) productivity was generally lower than today, but punctuated by episodes of surface phytoplankton blooms [*Thomas et al.*, 1995; *Rasmussen et al.*, 1996; *Nees et al.*, 1997; *Smart*, 2008; *Radi and de Vernal*, 2008]. These events were likely the result of changes in the position of the Arctic Front, which during past ice ages was shifted southward to latitudes between 42°–46°N [*Pflaumann et al.*, 2003]. Less information is available from lower latitudes or older time intervals. High-productivity events are recorded in sediments deposited during glacial Marine Isotope Stages (MIS) 8, 6 and 2 in the central North Atlantic between 37°–43°N [*Villanueva et al.*, 2001] and during MIS 16, 12, and 10 at IODP Site U1313 on the Mid-Atlantic Ridge, with the strongest productivity appearing during MIS 12 [*Stein et al.*, 2009]. In the western North Atlantic, episodes of surface phytoplankton blooms are documented during MIS 12 and MIS 10 at Site 1058 on the Blake Outer Ridge [*Poli et al.*, 2010], and tentatively linked to variability in the flow of the Gulf Stream and in particular to its meandering activity.

[6] On shorter timescales, large, rapid variations in primary productivity are associated with Heinrich (H) events, when massive discharges of icebergs from the ice sheets delivered cold, fresh water to the North Atlantic, enhancing surface water stratification, reducing the AMOC, and delivering ice rafted debris (IRD) to the ocean floor [e.g., *Broecker et al.*, 1992; *McManus et al.*, 2004]. At latitudes north of 40°N, these events are associated with a drastic decrease in primary productivity documented by low diatom abundances [*Rasmussen et al.*, 2002; *Nave et al.*, 2007]. By contrast, at the Bermuda Rise, at Site 607 on the mid-Atlantic Ridge, and in the SE Labrador Sea, IRD layers are associated with high diatom productivity [*Sancetta*, 1992; *Rasmussen et al.*, 2003; *Gil et al.*, 2009], probably stimulated by melting of icebergs and the consequent delivery of nutrients, especially silica and iron, and concurrent dilution of the surface ocean to retain more of these nutrients in the photic zone.

[7] In this paper we present the results of a study on sediments deposited on the Bermuda Rise (western subtropical North Atlantic) between ∼500 kyr and 340 kyr BP, a time interval extending from MIS 13 to MIS 10. The transition between MIS 12 and 11, commonly known as Termination V (∼424 ka), was a particularly dramatic glacial-interglacial change. During MIS 12 global ice volume was ∼15% greater than during the most recent glacial maximum (LGM), and sea level was ∼140 m lower than at present [*Rohling et al.*, 1998]. In contrast, MIS 11 was characterized by the warmest temperatures and the highest rates of North Atlantic Deep Water (NADW) production of the last 600,000 years [*Raymo et al.*, 1990; *Howard*, 1997]. The duration of the main warm

interval in MIS 11 (MIS 11.3) is estimated to have been ∼26–30 kyr, more than twice that of MIS 5e [*McManus et al.*, 2003; *Stein et al.*, 2009]. Beach deposits and elevated reef terraces indicate that sea level was as much as 20 m higher than the present-day during parts of MIS 11 [*Burckle*, 1997; *Hearty*, 1998; *Hearty et al.*, 1999; *Olson and Hearty*, 2009]. Thus, Termination V had a total sea level rise (∼160 m) approximately 30% greater than the sea level rise during the most recent deglaciation (∼120 m).

[8] Despite the extreme nature of the MIS 12–11 transition, MIS 11 (424–364 ka) is often considered the closest analog to the Holocene [*Loutre and Berger*, 2003; *de Abreu et al.*, 2005; *Ruddiman*, 2005]. Like the Holocene, the orbital parameters that prevailed during the early part of MIS 11 consisted of low eccentricity, high obliquity, and low precessional amplitude [*Berger and Loutre*, 1991; *Loutre and Berger*, 2003]. The long duration of the MIS 11.3 main warm interval noted by *McManus et al.* [2003] and *Stein et al.* [2009] is a consequence of the low eccentricity, which damps the precessional variations that produce cold stages [*Berger and Loutre*, 1991; *Berger et al.*, 1996]. Better understanding of the oceanic impacts of the transitions into MIS 11 and particularly out of this interglacial interval is important to improving predictions of future natural and human-influenced changes in climate.

[9] The objective of our study is to assess evidence of changes in marine productivity over the Bermuda Rise between ∼500 kyr and 340 kyr BP. Modern surface productivity in the area is low (∼140 g C m^{-2} y^{-1}) [*Helmke et al.*, 2010], but episodes of enhanced productivity have been recorded by *Gil et al.* [2009] during the last glacial and the Holocene. We utilize organic carbon mass accumulation rates and isotopic compositions of sediments deposited on the Bermuda Rise and their benthic foraminiferal assemblages as our paleoproductivity proxies. The combination of our proxies reveals significant variations in the amount and quality of organic matter delivered to Site 1063 throughout the study interval, including events of enhanced local surface productivity during glacial MIS 12 and the younger part of interglacial MIS 11, and we consider the paleoceanographic implications of these variations.

2. Site 1063 Environmental Setting and Sampling Strategy

2.1. Site 1063 Setting

[10] ODP Site 1063 (33°41′N, 57°37′W) is in 4595 m water on a sediment drift on the northeastern flank of the Bermuda Rise (Figure 1). This site lies within the present mixing zone between Antarctic Bottom Water (AABW) and the lower limb of North Atlantic Deep Water (LNADW). Sedimentation rates are high at this location, especially during glacial intervals, owing to advection of clay and silt into the region by deep recirculating gyres [*Keigwin and Jones*, 1994]. Site 1063 is presently located under the North Atlantic subtropical gyre, which is a pool of warm, low-nutrient water with low marine productivity. However, occasional injections of cold-core rings that are formed by Gulf Stream meanders evidently have created short episodes of higher productivity during the Holocene [*Gil et al.*, 2009]. Furthermore, southward repositioning of the Gulf Stream (Figure 1) and iceberg migrations during the most recent glacial and
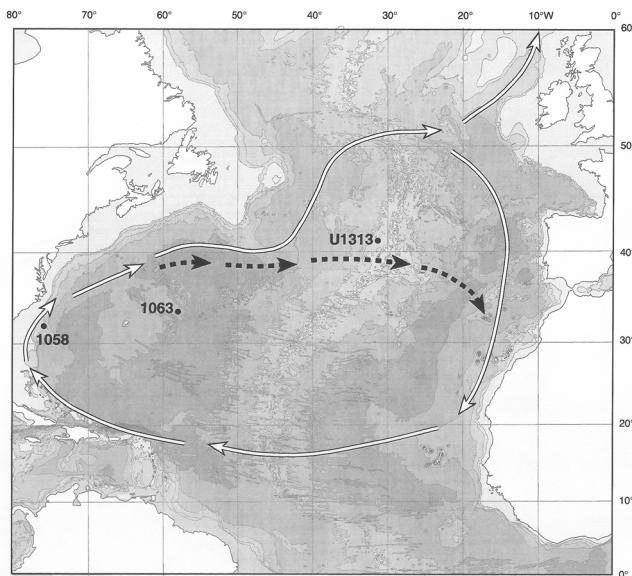
Figure 1. Location of ODP Site 1063 and other drilling sites important to this study. General surface circulation patterns of the modern (dark arrows) and glacial (dashed arrows) North Atlantic Ocean are shown.

deglacial intervals delivered nutrient-rich water that sustained higher productivity over this sector of the Bermuda Rise [*Gil et al.*, 2009].

2.2. Sampling

[11] Advanced hydraulic piston coring was used during ODP Leg 172 to recover sediment at Site 1063. The MIS 10–13 interval in the core was initially identified on the basis of the shipboard magnetic susceptibility record and the extinction of the calcareous nannofossil *Pseudoemiliania lacunosa*, which occurred within MIS 12 [*Thierstein et al.*, 1977]. The corresponding 31 m long composite section (approximately 76.9–108.4 mcd) consists of alternating nannofossil-rich and clay-rich sediments with variable silt contents [*Keigwin et al.*, 1998]. Samples (50 cm^3 in size) were collected at 7 cm intervals throughout this interval of the core.

3. Analytical Procedures

3.1. Age-Scale and δ^{18}O Stratigraphy

[12] Benthic foraminifera oxygen and carbon isotope data are from *Poli et al.* [2000] and were measured on the benthic foraminifer *Cibicidoides wuellerstorfi*. All analyses were performed on a VG Optima isotope ratio mass spectrometer equipped with an automated carbonate carousel. Samples were reacted at 90°C in phosphoric acid, and all isotope data are reported relative to Pee Dee belemnite (PDB) via the Carrara marble working standard.

[13] Our age model is based on the benthic foraminifera δ^{18}O stratigraphy (Figure 2). Seven time-control points were derived from the *Lisiecki and Raymo* [2005] stacked oxygen isotope record (Figure 2). Based on our interpretation of the oxygen isotope data, we conclude that our Site 1063 record extends from the lower part of MIS 10 (∼340 ka) to the upper part of MIS 13 (∼500 ka). Estimated sedimentation rates based on this chronology are high and extremely variable,

ranging from ∼7 cm/kyr during MIS 11 and up to 36 cm/kyr during MIS 10 (Figure 2), resulting in a sample temporal spacing ranging from 200 to 1,000 years.

3.2. Geochemical Analyses

3.2.1. Carbonate and Organic Carbon Contents

[14] The dried sediment samples were ground to a homogeneous powder with an agate mortar and pestle. Concentrations of calcium carbonate were determined using an automated, acid-digestion system at the University of South Carolina. Subsamples were treated with excess 3N HCl in the Marine Geology and Geochemistry Laboratory at the University of Michigan to remove their calcium carbonate contents in preparation for organic carbon analyses. The carbonate-free residue was recovered by centrifugation, rinsed to remove chlorides, and dried. The amount of total organic carbon (TOC) in the carbonate-free residue was determined with a Carlo Erba 1108 elemental analyzer. TOC concentrations are expressed on a whole-sediment basis after adjusting for the carbonate content of each sample. TOC/TN ratios were calculated on an atomic basis. TOC
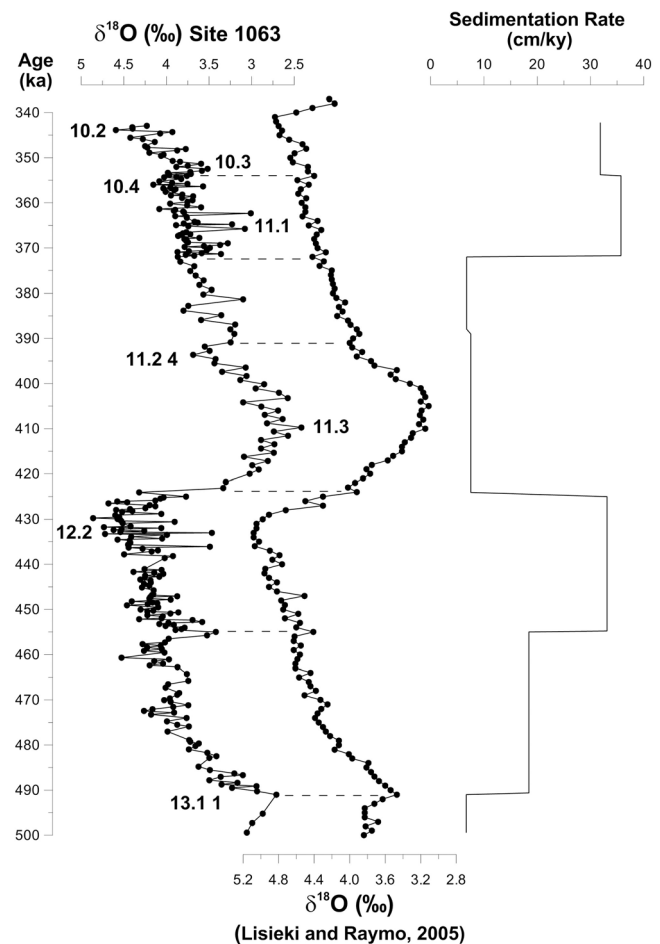

Figure 2. Age model for Site 1063 and resulting changes in linear sedimentation rates. The benthic foraminiferal oxygen isotope record was correlated to the *Lisiecki and Raymo* [2005] stacked oxygen isotope record. Dashed lines indicate tie points and numbers denote oxygen isotopic stages and substages labeled according to *Bassinot et al.* [1994].

mass accumulation rates (MARs) were calculated from the product of linear sedimentation rates (cm/kyr), the shipboard GRAPE bulk density (g/cm^3) and the TOC concentrations.

3.2.2. Organic Carbon Isotopes

[15] Portions of the carbonate-free residue were analyzed for their organic matter isotopic compositions in the Laboratory of Isotope Geochemistry at the University of Arizona using a Costech elemental analyzer interfaced directly with a Finnigan Delta Plus XL mass spectrometer. The $\delta^{13}C_{org}$ is given relative to the Vienna PeeDee Belemnite (VPDB) standard. Precision is better than ± 0.06‰.

3.2.3. Benthic Foraminiferal Analysis

[16] Approximately 45 cm^3 of each sample was dried in an oven at 40°C for 48 h, weighed, soaked in distilled water for 2 h, and then washed through a 63 μm sieve; the coarse fraction was dried and weighed. Assemblage analyses were carried out on the dry-sieved >125 μm fraction; samples were analyzed in their entirety, with the exception of nine samples from the MIS 11 interval and three samples from the MIS 13 interval, where the large number of individuals required the use of splits of approximately 300 specimens. Although the study of the >125 μm size fraction potentially underestimates the abundance of smaller but ecologically important species (e.g., *Epistominella exigua*), it has the advantage of allowing faster analysis of large sample sets while still showing major faunal patterns. A total of 42 benthic foraminiferal species were identified and counted. Benthic foraminiferal relative abundances were calculated for each species as percentage of the total assemblage. Species were identified by comparison with published illustrations and descriptions of modern foraminifera from the Atlantic Ocean (Table 1). We also calculated the absolute abundances of benthic foraminifera as number of specimens per gram of dry bulk sample, and the benthic foraminifera accumulation rates (BFAR) as number of individuals per gram of dry bulk sediment × linear sedimentation rates (cm/kyr) × GRAPE bulk density (gr/cm^3). For samples with more than 50 specimens, we determined the Shannon Information Index H(S) and the Species Equitability Index E, two indexes commonly used in studies of benthic foraminiferal assemblages and discussed in detail by *Gibson and Buzas* [1973]. In brief, H(S) is a measure of species number and evenness, and E is a measure of the relative abundance of each species. Equitability values range from 0, indicating high single-species dominance to 1, indicating equal abundance of all species. Paleoenvironmental interpretations of the foraminiferal assemblages are based on published ecological data for living foraminifera mainly from the North Atlantic, which are summarized in Table 1.

4. Results

4.1. TOC MARs and $\delta^{13}C_{org}$ Values

[17] TOC concentrations of the Site 1063 sediment sequence range from 0.2% to 0.7%, with all of the low values falling in the MIS 11 and 13 interglacials (Figure 3). Combined with the relatively high sedimentation rates in this sediment drift setting, these concentrations represent TOC MARs that vary between 0 and 2 g m^{-2} yr^{-1} in MIS 11 and 13 to 3.7 g m^{-2} yr^{-1} in MIS 12 (Figure 3). Highest concentrations and MARs appear in glacial substage 12.2. Nearly all of the atomic TOC/TN ratios fall between 6.5 and 10 (Figure 3). The higher values in this range are somewhat larger than in fresh algal organic matter (6–8) [*Jasper and Gagosian*, 1990; *Meyers*, 1994; *Geider and La Roche*, 2002], but they are similar to those found in some modern sediments where selective remineralization of nitrogenous components has elevated the initial TOC/TN ratios of marine organic matter [e.g., *Verardo and McIntyre*, 1994]. Moreover, none of the TOC/TN values approach those typical of land-plant organic matter (>20) [*Jasper and Gagosian*, 1990; *Meyers*, 1994]. Consequently, marine material appears to dominate the organic matter contents of the entire sediment sequence. Organic carbon $\delta^{13}C$ values fall in a relatively narrow range between ~ -25‰ and -22.5‰. The higher values appear in the sediments at the boundaries between interglacial stages 11 and 13 and the following glacial stages (Figure 3).

4.2. Benthic Foraminiferal Assemblages

[18] Benthic foraminiferal assemblages were analyzed in 225 samples. The total number of benthic foraminifera per sample varies between 1 and 1232, with 80 samples containing less than 50 individuals. These foram-poor samples are mainly from the intervals between 469 and 455 ka (MIS 12, 8 samples out of 18), 446.5–428 ka (MIS 12, 44 samples out of 50) and 366.5–356.5 ka (MIS 10, 11 samples out of 22) (diagonally stripped boxes in Figure 4). In these intervals, benthic foraminiferal test preservation is mediocre to good, and planktonic foraminiferal fragments are abundant to rare. Benthic foraminiferal preservation in all other samples is good to very good. Diatoms are common to abundant in the fraction >125 μm between 440 and 430 ka and 365–358 ka (green boxes with a capital D in Figure 4), in correspondence with layers of IRD (Figure 4) [*Poli et al.*, 2000] and samples with less than 50 benthic foraminiferal specimens. Radiolaria are present throughout MIS 12 and 10, with higher abundances during MIS 10. Silicoflagellates appear in only 6 samples, which are clustered between 450 and 440 ka, and they are rare. Pyritized burrows were found in 61 samples, and are particularly abundant during MIS 12.2 and MIS 10.4.

[19] Benthic foraminifera absolute abundances (BFAA) fluctuate between 0.02–27.8 tests per gram (Figure 4). Higher abundances (>10 tests/g) are recorded in late MIS 13, during most of MIS 11.3, and during late MIS 11 between ca. 385–374 ka, and in two samples at 352 ka. The lowest BFAA (<2 tests/g) are found during glacial MIS 12 between 446.5 and 428 ka and during glacial MIS 10.4 between 361 and 356 ka, in correspondence with diatom-rich intervals. Benthic foraminifera accumulation rates (BFAR), which are considered good proxies for past organic carbon fluxes to the ocean floor [e.g., *Herguera and Berger*, 1991; *Schmiedl and Mackensen*, 1997], vary between 1 and 552 tests cm^{-2} yr^{-1} and closely match the BFAA fluctuations (Figure 4). A significant positive correlation exists between BFAA and the concentration of CaCO$_3$ (r = 0.799, p < 0.001), and a positive correlation also exists between BFAR and %CaCO$_3$ (r = 0.414, p < 0.001). In the 120 samples where organic carbon data are available, a negative correlation is found between C$_{org}$ MAR and BFAA (r = −0.645, p < 0.001) and no significant correlation exists between C$_{org}$ MAR and BFAR (r = −0.124, p = 0.178) (Figure 5).

[20] The Shannon Information Index H(S) varies between 1.4 and 2.6. It shows significant, recurrent fluctuations between

Table 1. Species of Benthic Foraminifera Discussed in This Paper, With References to Figures and Ecological Preferences in the Literature

Species	Ecological Preferences
Alabaminella weddellensis (Earland), 1936 [*Gooday*, 1988, Figures 1d and 1e]	In association with *Epistominella exigua*, it is the most abundant species inhabiting phytodetritus. The phytodetritus assemblage appears to have low diversity and to be dominated by species that are uncommon in the underlying sediment [*Gooday*, 1988; *Smart and Gooday*, 1997].
	This species has relatively high abundances in subpolar latitudes of the North Atlantic Ocean (approximately N of 35°N) in correspondence with seasonally eutrophic waters, and in association with *Epistominella exigua* [*Sun et al.*, 2006].
	The relative abundances of *A. weddellensis* and *Epistominella exigua*, both of which have been described as species exploiting phytodetritus, are not always positively correlated. This indicates that they may have different ecological preferences, possibly utilizing different types of phytodetrital material [*Ohkushi et al.*, 1999; *Diz et al.*, 2007; *Smart*, 2008; *Smart et al.*, 2010].
Cibicidoides wuellerstorfi (Schwager), 1866 [*Jones*, 1994, Plate 93, Figures 8 and 9]	Epifaunal species that occupies elevated habitats and feeds on small organisms and detritus suspended in the water column [*Rasmussen et al.*, 2002].
	In the modern Atlantic Ocean, it is more common in carbonate-rich sediments in areas where the organic carbon flux to the seafloor is scarce, often coinciding with the presence of well-ventilated NADW [*Schnitker*, 1980; *Altenbach and Sarnthein*, 1989; *Mackensen et al.*, 1995].
	In the North Atlantic, relative abundances greater than 20% are found only where organic carbon fluxes are between 1 and 3 g m^{-2} yr^{-1} [*Altenbach et al.*, 1999].
	In the Equatorial tropical Atlantic off NW Africa it has been reported with abundances greater than 5% in areas where organic carbon fluxes are between 3 and 5 g m^{-2} yr^{-1} and bottom water oxygen concentration is greater than 3.0 ml/l [*Lutze and Coulbourn*, 1984; *Morigi et al.*, 2001].
Globocassidulina subglobosa (Bradyi), 1881 [*Jones*, 1994, Plate 54, Figure 17]	Higher abundances in areas characterized by relatively strong bottom currents [*Mackensen et al.*, 1995; *Schmiedl and Mackensen*, 1997; *Rasmussen et al.*, 2002].
	In the NE Atlantic and Antarctica, this species is associated with phytodetritus [*Smart*, 2008, and references therein]
Epistominella exigua (Brady), 1884 [*Gooday*, 1988, Figure 1f]	Very common in modern Northeast Atlantic deep waters; in the North Atlantic, below 3,000 m and south of 45°N, exceeds 10% of the total fauna [*Gooday*, 1993, and references therein].
	In association with *Alabaminella weddellensis*, this species has relatively high abundances in subpolar latitudes of the North Atlantic ocean (approximately N of 35°N) in correspondence with seasonally eutrophic waters [*Sun et al.*, 2006].
	Opportunistic species that colonizes and feeds on aggregates of phytodetritus produced by seasonal blooms of phytoplankton. This taxon quickly responds to the arrival of fresh food by rapidly reproducing, thus building up large populations [*Gooday*, 1988, 1993; *Smart et al.*, 1994; *Smart and Gooday*, 1997; *Thomas et al.*, 1995; *Fariduddin and Loubere*, 1997; *Fontanier et al.*, 2003].
Melonis barleeanum (Williamson), 1858 [*Katz and Miller*, 1987, Plate 4, Figure 6]	Common in upwelling areas where organic matter flux rates exhibit values between 3 and 6 g C$_{org}$ m^{-2} yr^{-1} and bottom water oxygen concentration is greater than 4.0 ml/l [*Schmiedl and Mackensen*, 1997; *Morigi et al.*, 2001].
	More abundant in the lower part of the sediment oxic zone where nitrate reduction occurs, and during times of high surface productivity. May prefer abundant but refractory organic matter, feeding either directly on the anaerobic bacteria that degrade the organic matter, or on the products of organic matter breakdown [*Licari et al.*, 2003; *Fontanier et al.*, 2003, and references therein].
	In laboratory experiments, the halt in supply of fresh organic material promoted an increase of the relative abundances of this species from rare (<0.5%) to common (2–9%), thus indicating that it is not dependent on regular supply of fresh organic material but utilizes refractory organic material and degradation products [*Alve*, 2010].
Melonis pompilioides (Fichtel and Moll), 1798 [*Jones*, 1994, Plate 109, Figures 10 and 11]	Infaunal taxon more abundant in areas with high surface productivity [*Mackensen et al.*, 1993; *Fariduddin and Loubere*, 1997].
Nuttallides umbonifera (Cushman), 1933 [*Carman and Keigwin*, 2004, Plate 1, Figures 1 and 2]	Abyssal epifaunal species adapted to environments characterized by scarce food supply and low bottom water temperature and salinity [*Gooday*, 1993; *Mackensen et al.*, 1995; *Loubere*, 1991].
	More common in areas bathed by bottom water masses very undersaturated with respect to carbonate; may be associated with AABW [*Bremer and Lohmann*, 1982; *Corliss et al.*, 1986; *Mackensen et al.*, 1995].
	In the NE Atlantic, dominates characterized by an oligotrophic food input regime that does not involve substantial pulses of phytodetritus [*Smart and Gooday*, 1997].
	Abundant in Holocene sediments of the Laurentian Fan (western North Atlantic) at depths of about 4,000 m, but absent from this area during the last glacial maximum when NADW was replaced by AABW; factors other than bottom water chemistry may affect the distribution of *N. umbonifer* [*Carman and Keigwin*, 2004].

Table 1. (continued)

Species	Ecological Preferences
Oridorsalis umbonatus (Reuss), 1851 [*Jones*, 1994, Plate 95, Figure 11, and Plate 105, Figure 2]	Cosmopolitan, epifaunal to shallow infaunal species more common in areas characterized by cold, well oxygenated bottom water where organic matter fluxes are generally low [*Mackensen et al.*, 1985; *Murgese and De Deckker*, 2005; *De and Gupta*, 2010]. In the Indian Ocean, thrives in well oxygenated, oligotrophic environments characterized by variable food supply [*De and Gupta*, 2010], or where the delivery of organic matter to the ocean floor is limited to specific periods [*Murgese and De Deckker*, 2005]. In the modern North Atlantic, this species is more common in sub-polar regions under seasonally eutrophic waters, in association with *Epistominella exigua* and *Alabaminella weddellensis* [*Sun et al.*, 2006]. In the eastern equatorial Pacific, it is one of the dominant species in areas of higher productivity [*Loubere*, 1991]. In the South Atlantic, *Mackensen et al.* [1995] report higher abundances of this taxon below zones of seasonally high surface production in water deeper than 2 km, and speculate a preference for low but sustained fluxes of highly degraded organic material. Dominates the assemblage in the Norwegian-Greenland Sea, where carbonate content is low [*Mackensen et al.*, 1985]; in the Sulu Sea, it is more common where bottom water carbonate saturation levels are high [*Miao and Thunell*, 1993]. Can tolerate low-oxygen conditions [*Rathburn and Corliss*, 1994; *Kaiho*, 1999].
Pullenia bulloides (d'Orbigny), 1826 [*Jones*, 1994, Plate 83, Figures 12 and 13]	Infaunal, found at depths between 1 and 4 cm below the seafloor, prefers intermediate to high organic carbon fluxes and low-oxygen conditions [*Gooday*, 1994; *Gupta and Thomas*, 1999; *Rathburn and Corliss*, 1994]. In the southern Atlantic Ocean, is associated with higher surface ocean productivity [*Mackensen et al.*, 1993]. In the South Atlantic, this species is indicative of high but seasonally varying surface productivity south of the Polar Front [*Mackensen et al.*, 1995]. In the equatorial Atlantic Ocean, it is associated with Intermediate flux of organic matter in areas bathed by NADW [*Fariduddin and Loubere*, 1997]. In the Pacific Ocean, is associated with areas of low productivity in the surface water and therefore low flux of organic matter to the seafloor [*Burke et al.*, 1993]. In the Indian Ocean, this species is indicative of low temperature, high oxygen and low food supply [*De and Gupta*, 2010].

490 and 460 ka and then consistently low values (below 1.8) in two intervals between approximately 430–445 ka and 360–375 ka. The equitability index E varies between 0.55 and 0.9, and shows a pattern similar to H(S).

[21] Benthic foraminiferal relative abundances were calculated in the 145 samples that had more than 50 individuals. Paleoenvironmental investigations should ideally be based on a minimum of 200–250 specimens. However, smaller numbers have been successfully used in studies on cores collected below 4,500m water depth, where the amount of benthic foraminifera is often small (e.g., 75 specimens [*Smart*, 2008]; 50 specimens [*Ishman*, 1996]).

[22] The three most common species are *Oridorsalis umbonatus* (>20% in 85 samples, mean 23.3%), *Nuttallides umbonifera* (>20% in 33 samples, mean 12.1%) and *Epistominella exigua* (>20% in 27 samples, mean 9.6%) (Figure 6). Relative abundances of these three species show significant variability throughout the investigated interval; to ensure that these are not the consequence of the "fixed sum" problem, we also calculated their absolute abundances (Figure 6). The results show a close match with relative abundance patterns, although BFAA changes are more subtle during the glacial intervals owing to the lower number of specimens in the samples. Two notable exceptions are evident between approximately 450–427 ka, where the percentage of *O. umbonatus* increases while its absolute abundance decreases, and between 370 and 355 ka, where *O. umbonatus* absolute abundance decreases while its

relative abundance remains high. Both intervals correspond with the highest recorded sedimentation rates (Figure 2), when all taxa undergo a decrease in absolute abundances. These discrepancies are probably the results of dilution of the benthic foraminiferal assemblage from enhanced fluxes of clastic sediment.

[23] Large changes in the relative abundances of *O. umbonatus* and *N. umbonifera* recur during early MIS 12 (approximately 490–455 ka), MIS 11.2 4–11.2 2 (~397–380 ka) and late MIS 10. *Oridorsalis umbonatus* dominates the assemblage during late MIS 12 (455–424 ka) and MIS 11.1–10.3 (380–350 ka), whereas *N. umbonifera* is the most abundant taxon during MIS 11.3. Large, rapid fluctuations in *E. exigua* percentages characterize early MIS 12 and the final part of MIS 11, between 382 and 362 ka. During MIS 11.3, this species is present in all samples with relative abundances <20%.

[24] Three additional species are present in most samples but at lower relative abundances than the species discussed above: *Globocassidulina subglobosa* (>20% in 16 samples, mean 9.6%), *Pullenia bulloides* (>20% in 8 samples, mean 6.6%), and *Cibicidoides wuellerstorfi* (>20% in 5 samples, mean 7.1%) (Figure 6). The percentages of all three taxa vary throughout the MIS 13–10 interval but lack a clear correlation with either glacial-interglacial climatic changes or organic carbon mass accumulation rates. Only *P. bulloides* shows slightly higher percentages between 426 and 397 ka
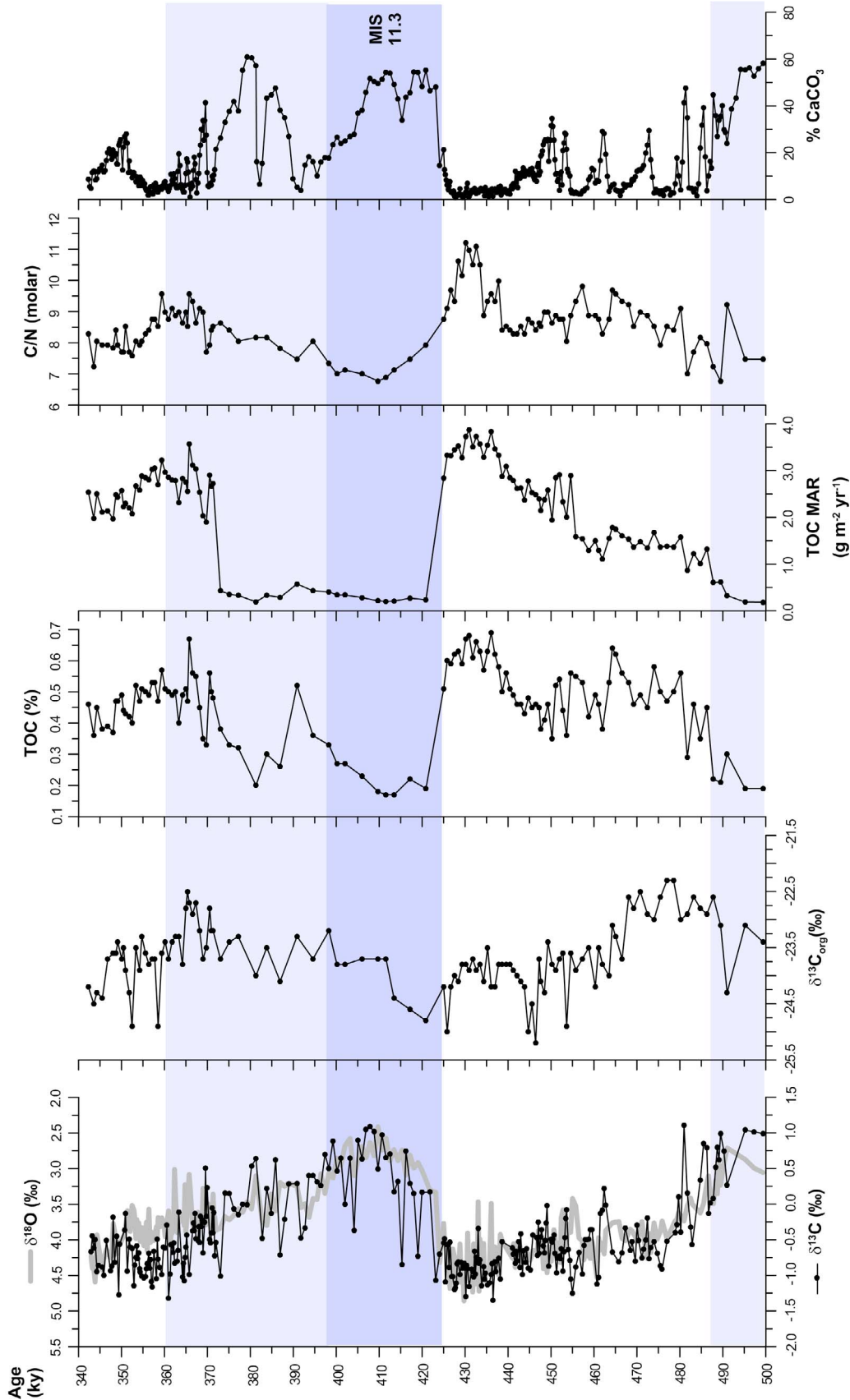
Figure 3. Different patterns of changes in paleoproductivity proxies in Site 1063 sediments deposited from 500 ka to 340 ka. Shaded areas highlight interglacial MIS 13 and 11; peak interglacial MIS 11.3 is emphasized with a darker shade. Carbonate $\delta^{13}C$ values are smaller in glacial MIS 12 and 10 than in interglacial MIS 11. Total organic carbon (TOC) concentrations and mass accumulation rates (MAR) peak during the terminations of MIS 12 and 11. Organic C/N ratios mimic TOC MAR variations and remain representative of marine organic matter. Organic $\delta^{13}C$ values are largest at onsets of MIS 12 and 10 and smallest at the onset of MIS 11. CaCO$_3$ concentrations are largest during MIS 11 and lowest during MIS 13 and 10. Carbonate data are from *Poli et al.* [2000].
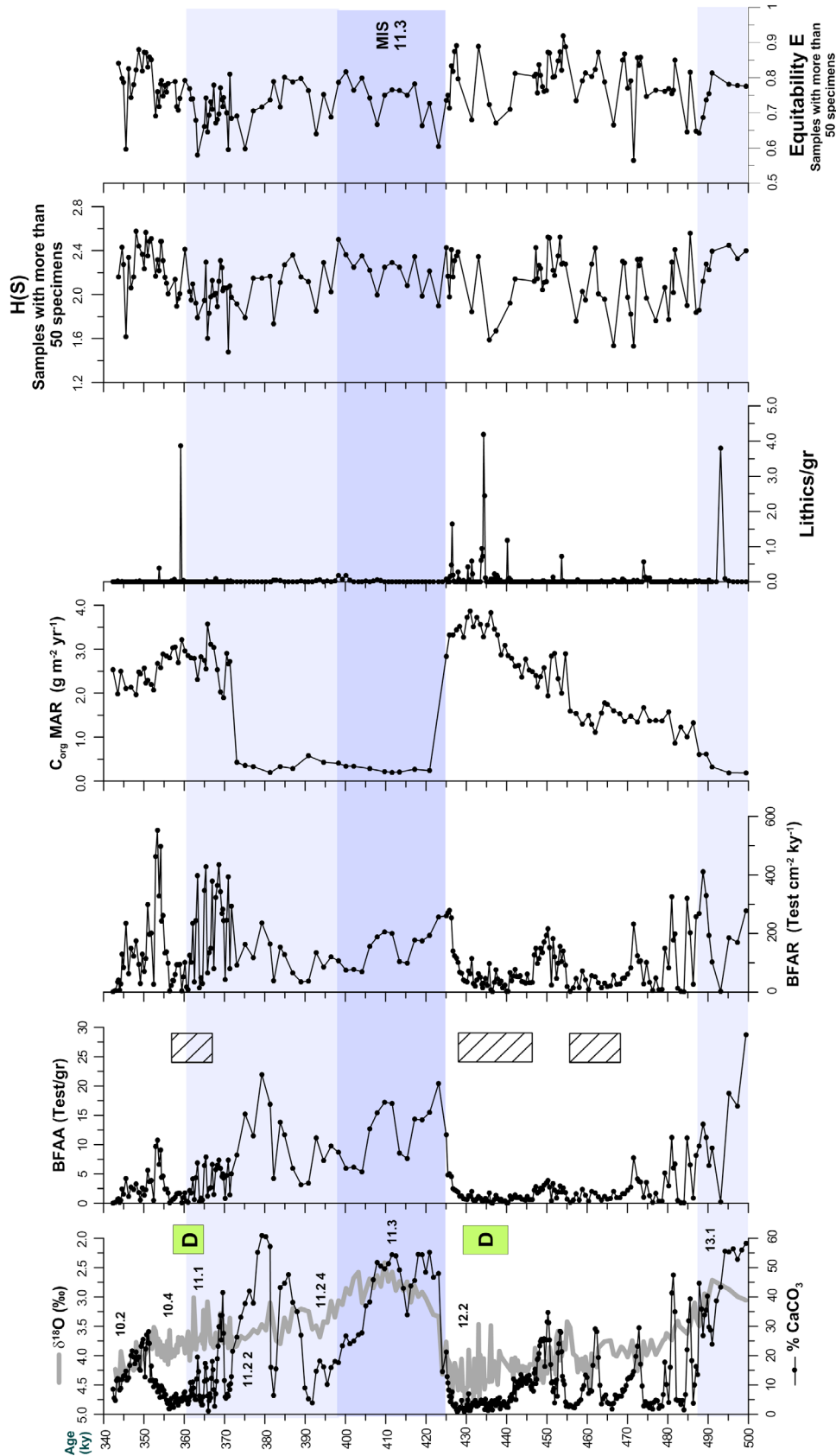
Figure 4. Changes in benthic foraminifera absolute abundances (BFAA), benthic foraminifera accumulation rates (BFAR), Shannon Information Index H(S) and Equitability E throughout the study interval. Benthic foraminiferal oxygen isotopes (thick gray line), calcium carbonate concentrations, organic carbon mass accumulation rates and layers of ice rafted debris (lithics/gr) are plotted as a reference. Diagonally stripped boxes outline intervals where several samples had less than 50 specimens of benthic foraminifera. BFAA and BFAR are higher during late MIS 13, most of MIS 11.3, and late MIS 11 between ca. 385–374 ka. Both are positively correlated with %CaCO$_3$, but not with organic carbon mass accumulation rates. Two green boxes with a capital D mark the position of diatom layers, which correspond to prominent IRD layers. Shaded areas highlight interglacial MIS 13 and 11; peak interglacial MIS 11.3 is emphasized with a darker shade.
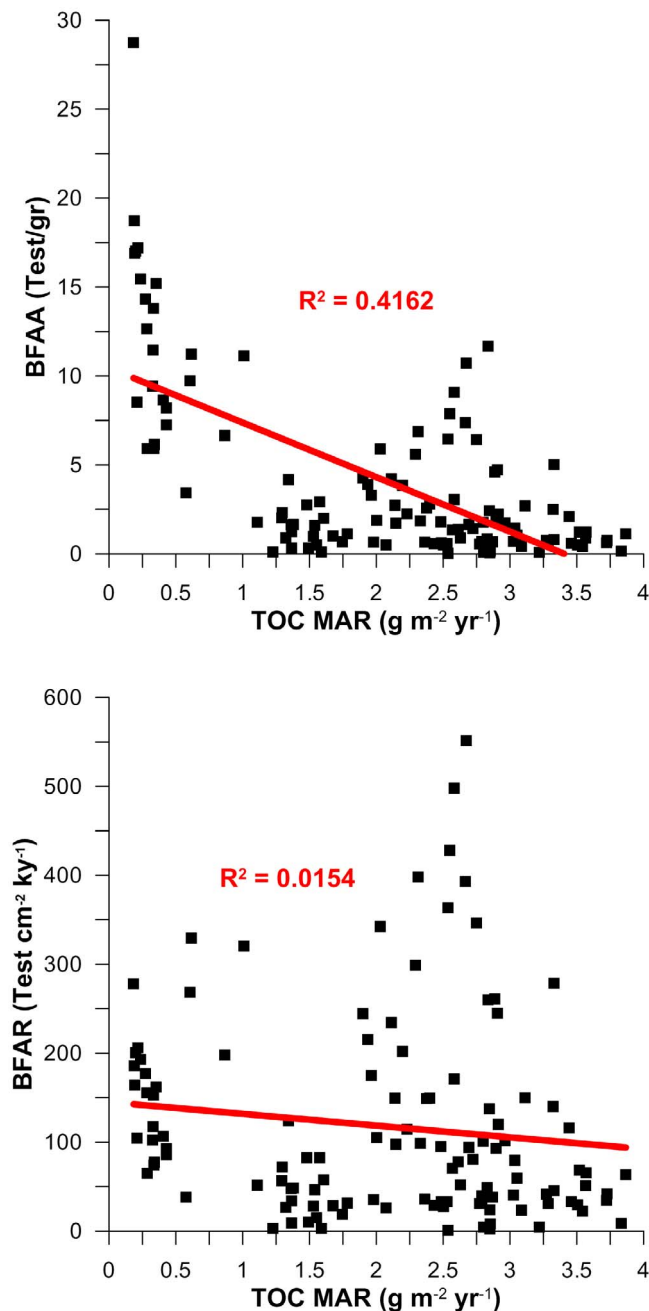
Figure 5. Crossplots of TOC MARs with benthic foraminiferal absolute abundances (BFAA) and benthic foraminiferal accumulation rates (BFAR), showing little correlation between the number of benthic fauna and organic matter accumulation, and indicating that the nature of the organic matter was not uniform over time.

(mean 13%; the mean is 9% between 490 and 426 ka and 3% between 397 and 352 ka).

[25] *Melonis pompilioides*, a species with generally low (<5%) relative abundances, shows higher percentages (5–20%) between 455 and 425 ka and 360–350 ka, in correspondence with higher organic carbon accumulation rates and a decline in the percentages of *E. exigua*. *Alabaminella weddellensis* reaches values >10% between 440 and 426 ka, an interval characterized by the presence of layers of diatoms

and IRD. Visual inspection of the 63–125 μm size fraction in these samples shows that *A. weddellensis* is abundant to very abundant, and hence our quantitative data likely underestimate the variability of this small species.

5. Interpretive Basis for Benthic Foraminifera at Site 1063

[26] Deep-sea benthic foraminiferal abundances and distribution patterns are significantly affected by the supply of organic matter. Indeed, a number of studies have successfully used BFAR as a proxy for past organic carbon fluxes to the seafloor [e.g., *Berger and Herguera*, 1992; *Herguera*, 2000; *Sun et al.*, 2006]. In our samples, a close correlation exists between BFAA, BFAR and %CaCO$_3$ (Figure 4). According to *Keigwin and Jones* [1994], late Quaternary calcite fluctuations on the Bermuda Rise are mainly driven by terrigenous dilution, rather than by changes in carbonate production or dissolution. Hence changes in the total number of benthic foraminifera per sample at Site 1063 are related to changes in terrigenous input rather than to variations in the amount of organic carbon delivered to the seafloor. The negative correlation between BFAA and C$_{org}$ MAR (Figure 5) and the low number of benthic foraminiferal tests in several samples from the intervals containing IRD and diatoms (Figure 4) indicate that dilution of the carbonate component is not driven solely by high terrigenous fluxes. Additionally, during the MIS 12 and 10 intervals in the Site 1063 sequence the presence of samples with few (<50) poorly preserved benthic foraminiferal tests, and common to abundant planktonic foraminiferal test fragments suggests that the carbonate assemblage has experienced significant dissolution. This process may originate at least partly from organic matter mineralization, but it could also be a consequence of enhanced influence of corrosive bottom water of southern origin [*Poli et al.*, 2000]. For these reasons, BFAA or BFAR at Site 1063 cannot be used to estimate past changes in export productivity of organic carbon. Therefore, our interpretation of the benthic foraminifera will be based on the ecological preferences of the most common species (summarized in Table 1) in the foraminiferal assemblages of the 145 samples where tests are well preserved.

[27] The three most abundant species, *N. umbonifera*, *O. umbonatus* and *E. exigua* (Figure 6) are commonly found in the modern North Atlantic Ocean at lower bathyal and abyssal depths [e.g., *Schnitker*, 1974, 1979, 1980; *Sun et al.*, 2006]. In our samples, no clear correlation exists between variations in the relative abundances of these taxa and benthic foraminiferal δ^{13}C changes (Figure 3). Hence faunal fluctuations cannot be attributed to preservation/dissolution cycles driven by changes in the corrosiveness of bottom water, but rather to changes in the amount and quality of organic matter reaching the seafloor.

[28] *Epistominella exigua* is a common epifaunal species in oligotrophic regions of the modern North Atlantic (see references in Table 1). Several studies on modern benthic assemblages show that this taxon colonizes and feeds on aggregates of phytodetritus, rapidly becoming the most abundant species of the benthic assemblage (Table 1). Phytodetritus consists of aggregates of phytoplankton and zooplankton remains bounded in a gelatinous matrix that is produced in the euphotic zone by spring phytoplankton
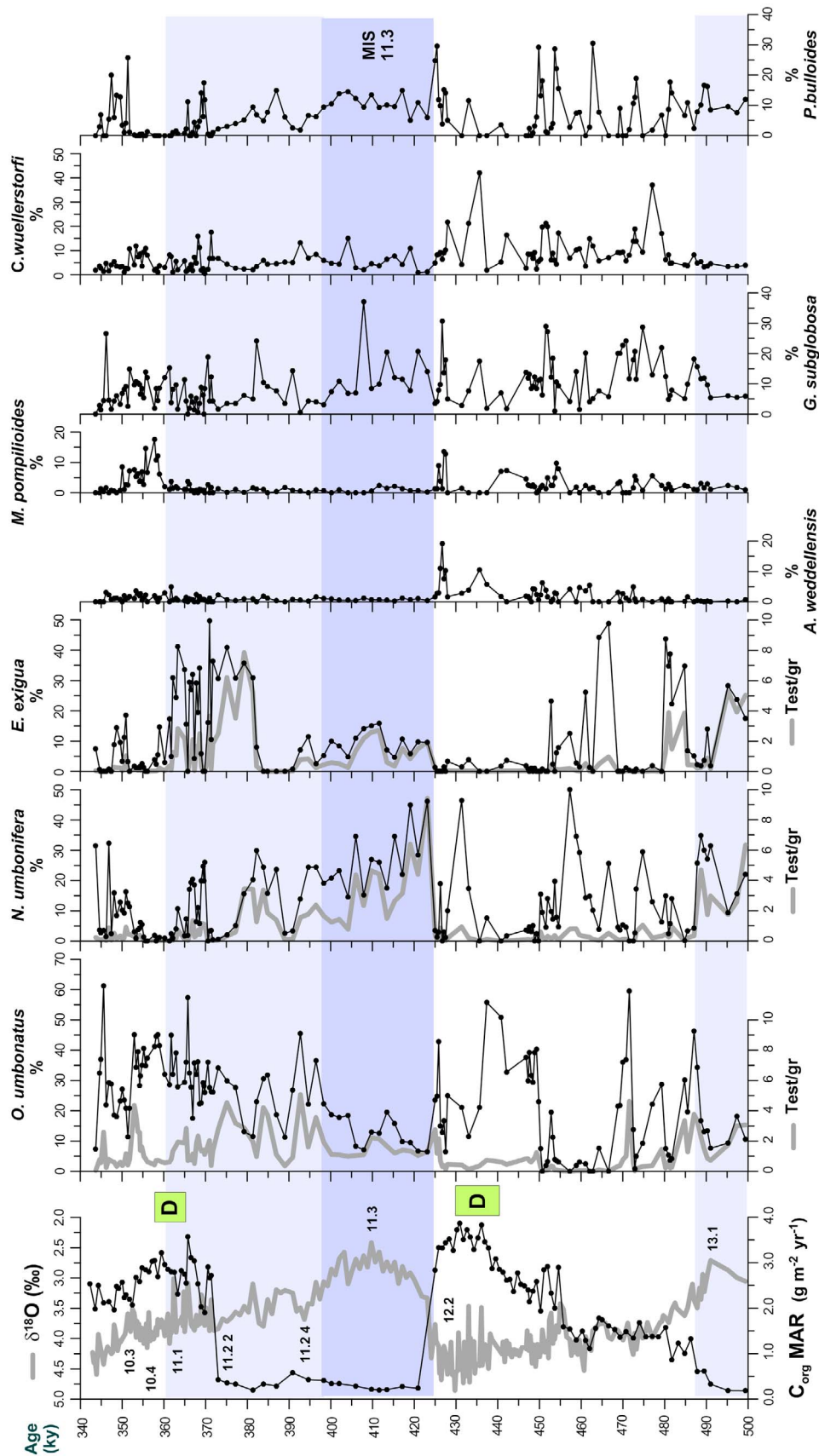
Figure 6. Relative abundances of the most common benthic foraminiferal taxa. Benthic foraminiferal oxygen isotopes (thick gray line) and organic carbon mass accumulation rates are plotted as a reference. The number of tests per gram is shown with a thick gray line in the graphs of *Oridorsalis umbonatus*, *Nuttallides umbonifera* and *Epistominella exigua*. Benthic foraminiferal assemblages are dominated by *N. umbonifera* during MIS 11.3 and indicate the presence of oligotrophic environments. High relative abundances of *O. umbonatus* during glacial intervals probably records the delivery of highly degraded organic material. Large, recurrent fluctuations in the abundance of *E. exigua* at the beginnings of the MIS 12 and MIS 10 record local episodes of phytoplankton blooms and consequent delivery of phytodetritus to the seafloor. Shaded areas highlight interglacial MIS 13 and 11; peak interglacial MIS 11.3 is emphasized with a darker shade. Two green boxes with a capital D mark the position of diatom layers. Numbers indicate oxygen isotope stages and substages according to *Bassinot et al.* [1994].

blooms, and it settles to the ocean floor at a rate of 100–150 m per day. The deposition of phytodetritus on the ocean floor delivers largely undegraded, labile organic carbon in areas that are otherwise characterized by low organic carbon fluxes [*Gooday*, 1993, and references therein]. This material is rapidly utilized by bacteria and foraminifera, and thus does not necessarily result in high sediment organic carbon accumulation rates [*Thomas et al.*, 1995; *Thomas and Gooday*, 1996; *Ohkushi et al.*, 1999]. Indeed, in our samples peak abundances of *E. exigua* (40–50%) are not always correlated with high TOC fluxes. We interpret the high abundances of this taxon during early MIS 12 (∼490–450 ka) and late MIS 11 (∼380–362 ka) as evidence of phytoplankton blooms at the surface and the consequent delivery of phytodetritus to the seafloor.

[29] *Nuttallides umbonifera* is an epifaunal species adapted to well oxygenated pore and bottom waters and extreme oligotrophic environments without significant delivery of phytodetritus (Table 1). *O. umbonatus* is a cosmopolitan shallow infaunal to epifaunal taxon that has been linked to several environmental factors, including different degrees of bottom water oxygenation and calcium carbonate saturation. In the modern oceans it is distributed in oligotrophic to moderately eutrophic areas, and in the North Atlantic it is associated with *E. exigua* and *A. weddellensis*, thus suggesting a preference for environments characterized by seasonally high surface productivity (Table 1). In the South Atlantic and the Weddell Sea, the distribution of this species overlaps with taxa indicative of high productivity and strong bottom currents, leading *Mackensen et al.* [1995] to speculate a preference for low but sustained fluxes of highly degraded organic matter. This hypothesis is supported by the frequent association of *O. umbonatus* with *Melonis barleeanum* and *M. pompilioides* [e.g., *Loubere*, 1991; *Mackensen et al.*, 1993; *Loubere*, 1996, *Gupta*, 1997; *Smart*, 2008], two closely related infaunal taxa that are more abundant under areas with high surface productivity, and that probably utilize refractory organic matter or the bacteria that degrade it (Table 1). If this interpretation is correct, high relative abundances of *O. umbonatus* in our samples document the delivery of refractory organic matter to Site 1063. Therefore, fluctuations in the relative abundance of *O. umbonatus* and *N. umbonifera* during early MIS 12 (before 455 kyr), MIS 11.2 4–11.2 2 (∼397–380 ka) and late MIS 10 are likely the result of episodic delivery of refractory organic matter in an environment that is otherwise characterized by mostly oligotrophic conditions.

[30] Persistently high abundances of *O. umbonatus*, low *N. umbonifera* percentages and the concurrent presence of *M. pompilioides* (3–10%) during late glacial MIS 12 (455–424 ka) and MIS 11.1–10.3 (377–350 ka) document enhanced delivery of degraded organic matter, in agreement with the organic carbon record showing significantly higher MARs in these intervals (>2 g C m^{-2} yr^{-1}) (Figure 6). By contrast, high abundances of *N. umbonifera* during the warmest part of MIS 11 (∼424–397 ka), with smaller amounts of *O. umbonatus* and *E. exigua* (both <20%) (Figure 6) document oligotrophic conditions similar to those found today under subtropical gyres, surface episodes of phytoplankton blooms, and the arrival of small amounts of degraded organic matter. Assuming that *E. exigua* percentages in the >125 μm fraction are a good proxy for seasonality of

primary productivity, our data indicate that seasonality was lower during MIS 11.3 than during early MIS 12 and late MIS 11.

[31] The Site 1063 benthic assemblage changes briefly between 437–431 ka, in correspondence with diatom-rich samples and an IRD layer and higher percentages of *A. weddellensis* (up to 20%, Figure 6), a small species that exploits phytodetritus and that is often found in association with *E. exigua* (Table 1). Studies of modern and fossil assemblages show that this taxon is better correlated with species indicative of high productivity than *E. exigua*, probably because the two taxa prefer different types of phytodetrital material (Table 1). Moreover, *A. weddellensis* is more common than *E. exigua* in Neogene diatom-rich sediments of the Pacific Ocean [*King et al.*, 1998]. Our data support a link between surface diatom blooms, higher organic carbon fluxes, and increased abundances of *A. weddellensis*.

[32] A second layer of diatoms and IRD is found at the transition from MIS 11 to MIS 10 (Figure 6). However, we do not find a concurrent increase in *A. weddellensis* abundances, and this taxon is also absent from the fine fraction (<125 μm) of our samples, thus indicating that the amounts and types of organic matter delivered to the benthic fauna differed during the two episodes of high productivity.

[33] *Globocassidulina subglobosa, P. bulloides* and *C. wuellerstorfi* are present throughout the study interval with relative abundances up to 30–40% (Figure 6). In the modern oceans, these species are more common in regions with well oxygenated bottom water, strong bottom currents and low surface productivity (Table 1). In the NE Atlantic and Antarctica, *G. subglobosa* is associated with phytodetritus. These taxa are present throughout the investigated interval, and they do not respond to the surface–ocean paleoclimatic changes recorded by other proxies. They are probably indicative of a well-ventilated deep water mass.

6. Bermuda Rise Paleoceanography During MIS 13–10

[34] Variations in organic carbon concentrations/accumulations and benthic foraminiferal assemblages indicate important glacial-interglacial changes in the amount and quality of organic matter delivered to the seafloor at Site 1063. Glacial periods MIS 10 and 12 are marked by TOC concentrations that are two to four times higher than those during interglacial periods (Figure 3). The low MIS 11 and MIS 13 TOC concentrations are similar to the average of 0.2% for modern pelagic sediments [*Degens and Mopper*, 1976], most of which are deposited under oligotrophic conditions. Because glacial and interglacial sedimentation rates at Site 1063 can differ by as much as an order of magnitude owing to their differences in advection of terrigenous sediment [*Keigwin and Jones*, 1994], we will henceforth employ MARs to discuss the differences in delivery of organic matter implied by the TOC concentrations.

6.1. Glacial-Interglacial Changes in the Amount and Quality of Organic Matter

[35] TOC MARs during glacial MIS 12 and MIS 11.1–10 are notably larger than those in the interglacial sections, ranging between 0.7 to 3.7 g m^{-2} yr^{-1}. These values are similar to those presently found in sediments beneath the

California Current upwelling zone (2.2 g C m^{-2} yr^{-1}) [*Suess and Müller*, 1980]. The dominance of *O. umbonatus* in correspondence with TOC MARS >0.2 g m^{-2} yr^{-1} indicates the delivery of low quality organic matter at these times, and hence the elevated TOC MARs are likely related to enhanced delivery of terrigenous sediment during these intervals, as documented by the high sedimentation rates (>30 cm/kyr, Figure 3). The higher sedimentation rates would cause faster burial and associated greater preservation of organic matter, which is expressed in the elevated TOC MARs.

[36] Site 1063 is presently under the North Atlantic subtropical gyre, which is an area of low surface productivity (~140 g C m^{-2} y^{-1}) [*Helmke et al.*, 2010] because of weak vertical mixing resulting from strong water column stratification. Regions of high productivity are found north of the site, in association with the Arctic Front. Here, recurrent eddy formation along the northern edge of the Gulf Stream induces upwelling that fuels episodes of high primary production [*Yoder et al.*, 1981, 1994; *Lee et al.*, 1991; *Gil et al.*, 2009]. During the Last Glacial Maximum, the Arctic Front - Gulf Stream boundary shifted southward to about 40°N [*Pflaumann et al.*, 2003] and closer to Site 1063 (Figure 1). At the same time, lower sea level resulted in greater supply of sediment to the Bermuda Rise, mostly originating from off Nova Scotia [e.g., *Keigwin and Jones*, 1989]. This process increased sedimentation rates and delivered fine grained carbonate (<63 μm), alkenones and organic carbon up to 7,000 years older than coexisting planktonic foraminifera (>150 μm), which are autochthonous [*Ohkouchi et al.*, 2002]. Indeed, *Schnitker* [1979] documented higher abundances of *M. pompilioides* in core GPC-5 (Bermuda Rise) at this time, a taxon associated with high fluxes of refractory organic matter (Table 1). Primary productivity off Nova Scotia during the LGM has been estimated between 250 and 350 g C m^{-2} yr^{-1}, which is higher than at most northern latitudes at that time, although slightly lower than today [*Radi and de Vernal*, 2008]. Therefore, higher abundances of *M. pompilioides* during the LGM at core GPC-5 probably reflect enhanced erosion of shallow water sediments at higher latitudes, rather than enhanced primary productivity in the North Atlantic.

[37] We hypothesize that southward displacement of the Arctic Front – Gulf Stream during MIS 12 and enhanced lateral advection of fine-grained material from higher latitudes, similar to the last glacial interval, are the most probable causes of the observed changes in glacial-stage organic carbon accumulation and benthic foraminiferal assemblages at Site 1063. According to our data, organic matter produced along the Arctic Front was occasionally entrained in the flow of deep sea currents during early MIS 12 and eventually delivered to the Bermuda Rise, resulting in significant fluctuations in the abundances of *O. umbonatus*. In the upper part of MIS 12 (~455–437 ka) and MIS 11.1–10, consistently high abundances of *O. umbonatus* and higher % *M. pompilioides* are likely the result of a higher and sustained flux of refractory organic matter, probably related to the southward shift of the Arctic Front and enhanced delivery of fine material to Site 1063. In fact, episodes of enhanced surface productivity in the North Atlantic at this time are documented by an increase in alkenone concentrations at Site U1313 (41°N, 32.57°W, Figure 1 and Figure 7) [*Stein et al.*, 2009], and by high relative abundances of *Turborotalita quinqueloba* (>50%) at Site U1314 (56°21.8′N, 27°53.3′W)

[*Alonso-Garcia et al.*, 2011]. Both are attributed to a more southern position of the Arctic Front.

[38] TOC MARs in the first part of MIS 11 (420–372 ka) and the small portion of middle MIS 13 (484–480 ka) that our sampling captured are between 0.2 and 0.5 g C m^{-2} yr^{-1} (Figure 3). Although these values are two orders of magnitude higher than under present-day open-ocean gyres (3 mg C m^{-2} yr^{-1}) [*Suess and Müller*, 1980], we interpret them to reflect the high sedimentation rates (~7 cm/kyr) that persisted at Site 1063 even during interglacial periods and increased delivery of advected organic matter produced at more northerly locations, rather than evidence of high surface productivity.

[39] The Site 1063 MIS 11.3 benthic fauna assemblage, which is dominated by *N. umbonifera*, documents the establishment of oligotrophic conditions similar to those found during the Holocene part of core GPC 5 [*Schnitker*, 1979]. However, during MIS 11.3 *O. umbonatus* percentages vary between 5 and 20%, while this taxon is not present with significant abundances during the Holocene [*Schnitker*, 1979]. This contrast indicates that the delivery of degraded organic matter from higher latitudes was higher during MIS 11.3 than during the last 10 kyr. This difference may be the result of warmer temperatures and reduced sea ice cover during MIS 11.3, which would have enhanced primary productivity at high latitudes by increasing light availability, a scenario projected by climate models under conditions of continued global warming [e.g., *Steinacher et al.*, 2010].

6.2. Episodes of Surface Phytoplankton Blooms

[40] Recurrent episodes of surface phytoplankton blooms are documented by high relative abundances of *E. exigua* during early MIS 12 and late MIS 11 and by two diatom layers, the oldest of which is associated with higher percentages of *A. weddellensis* (Figure 5). As previously discussed, both *E. exigua* and *A. weddellensis* are taxa that exploit phytodetritus, and high abundances of either or both these species in fossil assemblages have been interpreted as evidence of seasonal events of primary productivity (Table 1). However, *Sun et al.* [2006] found that in the North Atlantic the sum of the relative abundance of the two species (the "Phytodetrital Group") correlates with seasonality of productivity, while percentages of either species alone does not. At Site 1063, percentages of the "Phyodetrital Group" vary between 0 and 53%, and the estimated seasonality index varies between 0–0.45 (Figure 8), with higher values (>0.3) and hence likely stronger seasonality, between 490 and 460 ka, and 380–360 ka. These intervals are characterized by lower diversity H(S) and equitability E (Figure 4), which also point to higher seasonality [*Corliss et al.*, 2009]. A comparison with the seasonality index map of the North Atlantic developed by *Sun et al.* [2006] shows that modern values in the Bermuda Rise area (~0.3) are close to our highest values, while the MIS 11.3 index is significantly lower than today's. This difference is most probably the result of the different size fractions investigated (>125 μm in this paper, and >63μm in *Sun et al.* [2006]), and hence the Site 1063 data should be considered minimum values.

[41] Events of significant phytoplankton bloom at the Bermuda Rise are also documented during the last 23 kyr [*Schnitker*, 1979]. During the Last Glacial Maximum, *E. exigua* abundances fluctuate between 30 and 76%, which
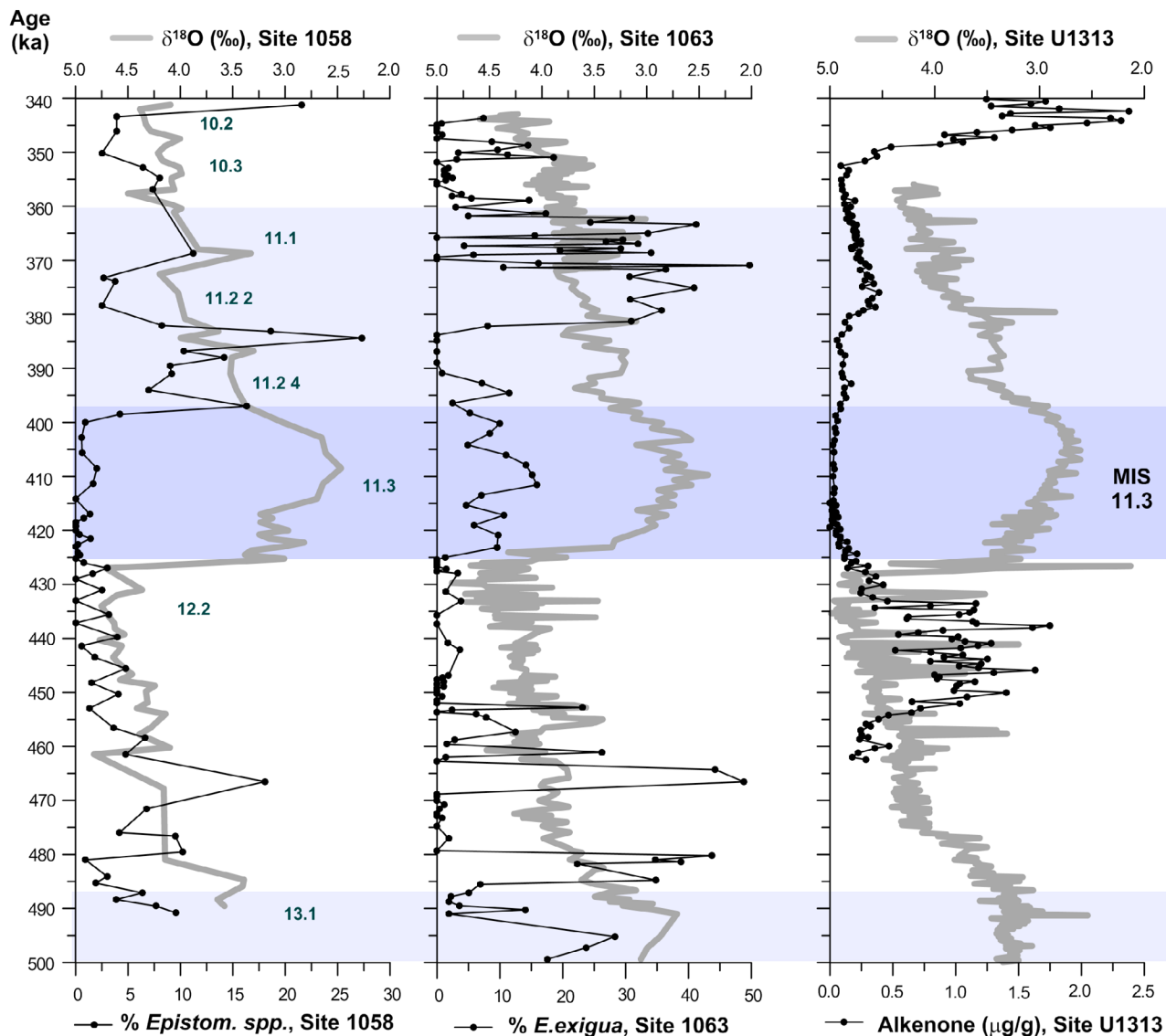
Figure 7. Comparison of primary productivity proxies at Site 1058, 1063 and U1313.

is within the range recorded at Site 1063. During the Holocene, *E. exigua* percentages reach values close to 40% in two samples, thus suggesting that during the last 10 kyr seasonality was at times higher than during MIS 11.3. This difference may be the result of warmer temperatures and stronger thermal stratification during MIS 11.3, which is also an expected consequence of future global warming [e.g., *Polovina et al.*, 2008].

[42] During the MIS 10–13 time interval, episodes of enhanced surface productivity are inferred from high *E. exigua* abundances at the Blake Outer Ridge (ODP Site 1058, Figure 1 and Figure 7) and are ascribed to meanders of the Gulf Stream [*Poli et al.*, 2010]. Fluctuations in the relative abundances of this taxon at Site 1058 are not as large as at the Bermuda Rise, documenting weaker phytoplankton blooms along the continental margin. These events appear to be synchronous at the two sites during MIS 12, but not during MIS 11.2 4–10.2, when episodes of phytoplankton blooms begin earlier at Site 1058 (shortly after the termination of MIS 11.3) than at Site 1063. Alkenone concentration records

from Site U1313 on the Mid-Atlantic Ridge document significant changes in nannoplankton productivity during MIS 12.2 and MIS 10.2, and hence later than at Site 1063 and 1058 (although the MIS 12 record of Site U1313 starts at 460 ka).

[43] The different timing of these productivity events is not an artifact of the age models used in the three investigations; Site 1063 and Site U1313 age models are based on the oxygen isotope stack of *Lisiecki and Raymo* [2005], which during MIS 11 and 10 is similar to the low latitude oxygen isotope stack of *Bassinot et al.* [1994] used for Site 1058. Assuming that the position of the Arctic Front during MIS 11.3 was similar to today, we speculate that the three sites trace the progressive southward displacement of the Arctic Front and related shift of the path of the Gulf Stream during the global cooling that followed the termination of MIS 11.3. Site 1058, being closer to the northern boundary of the Gulf Stream, was affected first, while Site U1313 was affected last.
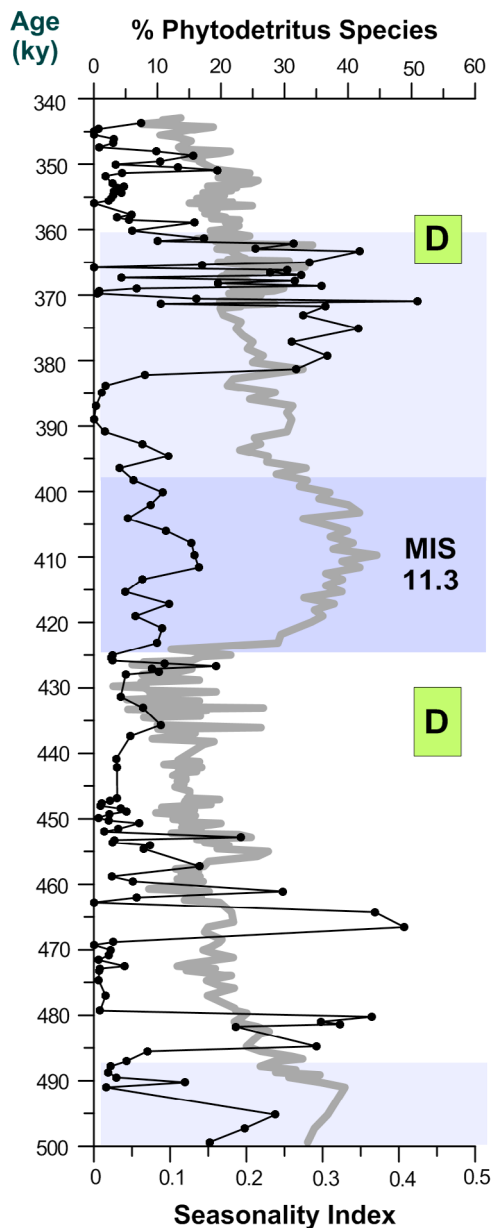
Figure 8. Percentages of "Phytodetritus Species." The seasonality index was estimated following *Sun et al.* [2006, Figure 9b]. Benthic foraminiferal oxygen isotopes (thick gray line) are plotted as a reference.

[44] Two diatom rich layers centered around 435 ka and 355 ka document important events of primary productivity at the Bermuda Rise. In the modern ocean, diatom blooms are usually associated with upwelling zones. However, in our samples the increase in diatom production is associated with the presence of IRD, thus suggesting a correlation with the arrival of icebergs. The concurrent presence of diatom-rich intervals and IRD at the Bermuda Rise has recently been documented in correspondence with Heinrich (H) event 1, 2 and 3 [*Gil et al.*, 2009; *Lippold et al.*, 2009]. According to *Gil et al.* [2009] higher diatom productivity during H1 results from the combined presence of cold-core rings shed by the Gulf Stream, eddies of southern origin and nutrient-rich

iceberg meltwater, which potentially contributes iron to the phytoplankton [*Smith et al.*, 2007; *Schwarz and Schodlok*, 2009]. In our samples diatoms are found toward the end of high productivity intervals documented by TOC MARs and benthic assemblages (Figure 6), thus showing that ice melting enhanced a process that had been underway for several thousand years.

[45] Higher abundances of *A. weddellensis* are associated with the older diatom layer, but not with the younger one. This difference is consistent with geochemical evidence that both the amounts and types of organic matter that were delivered to the benthic fauna differed during the two episodes of high productivity. TOC MARs associated with the MIS 12 diatom layer are the highest in the whole sequence $(3.7 \, \mathrm{g \, C \, m^{-2} \, yr^{-1}})$, whereas they are $2.9 \, \mathrm{g \, C \, m^{-2} \, yr^{-1}}$ during the MIS 10 diatom bloom. Similarly, the C/N values found in the MIS 12 diatom layer are as high as 11.5, but those in the MIS 10 layer are $\sim$9 (Figure 3), which indicate greater degradation of the organic matter [*Prahl et al.*, 1997] and hence diminished nutritional value to the benthic fauna.

7. Summary and Conclusions

[46] We have studied geochemical and microfossil evidence for changes in marine productivity in sediments deposited between 500 and 340 ka at ODP Site 1063 on the Bermuda Rise. This period of time includes the end of interglacial MIS 13, glacial MIS 12, Termination V, interglacial MIS 11, and the start of glacial MIS 10. Organic carbon mass accumulation rates and isotopic compositions and the benthic foraminiferal assemblages of a suite of high-resolution sediment samples are our paleoproductivity proxies. We summarize here the results of our study of this western subtropical North Atlantic site.

[47] 1. During MIS 11.3 benthic foraminiferal assemblages document the presence of oligotrophic conditions at the Bermuda Rise and the delivery of small amounts of refractory organic matter, probably of northern origin. The amount of organic matter reaching this region was higher than during the Holocene, probably reflecting enhanced productivity at higher latitudes due to reduced ice cover during this particularly warm interglacial. Our data also document lower relative abundances of *E. exigua* at this time than during the Holocene, thus suggesting stronger stratification of the upper water column and reduced episodes of phytoplankton blooms during MIS 11.3.

[48] 2. Glacial MIS 12 and the MIS 11.2 4–10 intervals are characterized by higher fluxes of degraded organic matter which are initially intermittent and then become steadier. This material was likely produced in proximity of the Arctic Front, which during these cold intervals was displaced south of its modern position and closer to Site 1063, in a manner similar to that described during the Last Glacial Maximum.

[49] 3. The early part of MIS 12 and the MIS 11.2–10 intervals are marked by frequent, intermittently high episodes of phytoplankton blooms at the surface, documenting the southward migration of the Gulf Stream and related eddy activity. Similar events are recorded at other sites in the North Atlantic, although they appear to occur earlier at lower latitudes in the western North Atlantic, and several thousand years later at higher latitudes in the central North Atlantic.

These time-transgressive events likely document a complex movement of the Arctic Front – Gulf Stream system in different regions of the North Atlantic.

[50] 4. Diatom remains found in correspondence with two IRD layers near the terminations of MIS 12 and MIS 10 document episodes of enhanced diatom productivity related to iceberg melting.

[51] The results of our study substantiate previous studies that have described profound paleoceanographic changes in the North Atlantic Ocean over glacial-interglacial cycles and that have found evidence of the southward migration of the Gulf Stream during glacial intervals. They also confirm findings that these changes were magnified between MIS 12 and 11 because of the strong paleoclimatic contrast between these two stages. The present interglacial stage has been predicted to be very similar to the extended MIS 11.3 warm interval (27 kyr), during which we found a strong shift to oligotrophic conditions at Site 1063. The additional climate warming anticipated in the future because of anthropogenic pCO_2 increases is likely to cause even greater oceanographic changes than we found during the natural transition from MIS 12 to MIS 11.

References

Alonso-Garcia, M., F. J. Sierro, and J. A. Flores (2011), Arctic front shifts in the subpolar North Atlantic during the Mid-Pleistocene (800–400 ka) and their implications for ocean circulation, *Palaeogeogr. Palaeoclimatol. Palaeoecol.*, 311(3–4), 268–280, doi:10.1016/j.palaeo.2011.09.004.

Altenbach, A. V., and M. Sarnthein (1989), Productivity record in benthic foraminifera, in *Productivity of the Ocean: Present and Past*, edited by W. H. Berger, V. S. Smetaceck, and G. Wefer, pp. 255–269, Wiley, Chichester, U. K.

Altenbach, A. V., U. Pflauman, R. Schiebel, A. Thies, S. Timm, and M. Trauth (1999), Scaling percentages and distributional patterns of benthic foraminifera with flux rates of organic carbon, *J. Foraminiferal Res.*, 29(3), 173–185.

Alve, E. (2010), Benthic foraminiferal responses to absence of fresh phytodetritus: A two year experiment, *Mar. Micropaleontol.*, 76, 67–75, doi:10.1016/j.marmicro.2010.05.003.

Antoine, D., J.-M. Andre, and A. Morel (1996), Oceanic primary production. Estimation at global scale from satellite (coastal zone color scanner) chlorophyll, *Global Biogeochem. Cycles*, 10, 57–69, doi:10.1029/95GB02832.

Bassinot, F. C., L. D. Labeyrie, E. Vincent, X. Quidelleur, N. J. Shackleton, and Y. Lancelot (1994), The astronomical theory of climate and the age of the Brunhes-Matuyama magnetic reversal, *Earth Planet. Sci. Lett.*, 126, 91–108, doi:10.1016/0012-821X(94)90244-5.

Berger, A., and M. F. Loutre (1991), Insolation values for the climate of the last 10 million years, *Quat. Sci. Rev.*, 10(4), 297–317, doi:10.1016/0277-3791(91)90033-Q.

Berger, W. H., and J. C. Herguera (1992), Reading the sedimentary record of the ocean's productivity, in *Primary Productivity and Biogeochemical Cycles in the Sea*, edited by P. G. Falkowski and A. D. Woodhead, pp. 455–486, Plenum, New York.

Berger, W. H., T. Bickert, M. K. Yasuda, and G. Wefer (1996), Reconstruction of atmospheric CO_2 levels from ice-core data and the deep-sea record of Ontong Java plateau: The Milankovitch Chron, *Geol. Rundsch.*, 85, 466–495, doi:10.1007/BF02369003.

Bremer, M. L., and G. P. Lohmann (1982), Evidence for primary control on the distribution of certain Atlantic Ocean benthonic foraminifera by degree of carbonate saturation, *Deep Sea Res., Part A*, 29, 987–998, doi:10.1016/0198-0149(82)90022-X.

Broecker, W. S. (1982), Glacial to interglacial changes in ocean chemistry, *Prog. Oceanogr.*, 11, 151–197, doi:10.1016/0079-6611(82)90007-6.

Broecker, W. S., G. C. Bond, M. Klas, E. Clark, and J. F. McManus (1992), Origin of the North Atlantic's Heinrich Events, *Clim. Dyn.*, 6, 265–273, doi:10.1007/BF00193540.

Burckle, L. H. (1997), Oxygen isotope stage 11 warming, *EOS Trans. AGU*, 78(17), Spring Meet. Suppl., OS21B-01.

Burke, S. K., W. H. Berger, W. T. Coulbourn, and E. Vincent (1993), Benthic foraminifera in box core ERDC 112, Ontong Java Plateau, *J. Foraminiferal Res.*, 23, 19–39, doi:10.2113/gsjfr.23.1.19.

Carman, M. R., and L. D. Keigwin (2004), Preservation and color differences in *Nuttallides umbonifera*, *J. Foraminiferal Res.*, 34(2), 102–108, doi:10.2113/0340102.

Corliss, B. H., D. G. Martinson, and T. Keffer (1986), Late Quaternary deep-ocean circulation, *Geol. Soc. Am. Bull.*, 97, 1106–1121, doi:10.1130/0016-7606(1986)97<1106:LQDC>2.0.CO;2.

Corliss, B. H., C. W. Brown, X. Sun, and W. J. Showers (2009), Deep-sea benthic diversity linked to seasonality of pelagic productivity, *Deep Sea Res., Part I*, 56(5), 835–841, doi:10.1016/j.dsr.2008.12.009.

De, S., and A. K. Gupta (2010), Deep-sea faunal provinces and their inferred environments in the Indian Ocean based on distribution of recent benthic foraminifera, *Palaeogeogr. Palaeoclimatol. Palaeoecol.*, 291, 429–442, doi:10.1016/j.palaeo.2010.03.012.

de Abreu, C., F. F. Abrantes, N. J. Shackleton, P. C. Tzedakis, J. F. McManus, D. W. Oppo, and M. A. Hall (2005), Ocean climate variability in the eastern North Atlantic during interglacial marine isotope stage 11: A partial analogue to the Holocene?, *Paleoceanography*, 20, PA3009, doi:10.1029/2004PA001091.

Degens, E. T., and K. Mopper (1976), Factors controlling the distribution and early diagenesis of organic material in marine sediments, in *Chemical Oceanography*, edited by J. P. Riley and R. Chester, pp. 59–113, Academic, London.

Diz, P., I. R. Hall, R. Zahn, and E. G. Molyneux (2007), Paleoceanography of the southern Agulhas Plateau during the last 150 ka: Inferences from benthic foraminiferal assemblages and multispecies epifaunal carbon isotopes, *Paleoceanography*, 22, PA4218, doi:10.1029/2007PA001511.

Fariduddin, M., and P. Loubere (1997), The surface ocean productivity response of deeper water benthic foraminifera in the Atlantic Ocean, *Mar. Micropaleontol.*, 32, 289–310, doi:10.1016/S0377-8398(97)00026-1.

Field, C. B., M. J. Behrenfeld, J. T. Randerson, and P. Falkowski (1998), Primary production of the biosphere: Integrating terrestrial and oceanic components, *Science*, 281, 237–240, doi:10.1126/science.281.5374.237.

Fontanier, C., F. J. Jorissen, G. Chailloua, C. David, P. Anschutz, and V. Lafon (2003), Seasonal and interannual variability of benthic foraminiferal faunas at 550 m depth in the Bay of Biscay, *Deep Sea Res., Part I*, 50(4), 457–494, doi:10.1016/S0967-0637(02)00167-X.

Geider, R. J., and J. La Roche (2002), Redfield revisited: Variability of C: N: P in marine microalgae and its biochemical basis, *Eur. J. Phycol.*, 37(1), 1–17, doi:10.1017/S0967026201003456.

Gibson, T. G., and M. A. Buzas (1973), Species diversity: Patterns in modern and Miocene Foraminifera of the Eastern Margin of North America, *Geol. Am. Bull.*, 84, 217–238, doi:10.1130/0016-7606(1973)84<217:SDPIMA>2.0.CO;2.

Gil, I. M., L. D. Keigwin, and F. G. Abrantes (2009), Deglacial diatom productivity and surface ocean properties over the Bermuda Rise, northeast Sargasso Sea, *Paleoceanography*, 24, PA4101, doi:10.1029/2008PA001729.

Gooday, A. J. (1988), A response by benthic foraminifera to the deposition of phytodetritus in the deep sea, *Nature*, 332, 70–73, doi:10.1038/332070a0.

Gooday, A. J. (1993), Deep-sea benthic foraminiferal species which exploit phytodetritus: Characteristic features and controls on distribution, *Mar. Micropaleontol.*, 22, 187–205, doi:10.1016/0377-8398(93)90043-W.

Gooday, A. J. (1994), The biology of deep-sea foraminifera: A review of some advances and their applications in paleoceanography, *Palaios*, 9, 14–31, doi:10.2307/3515075.

Gupta, A. K. (1997), Paleoceanographic and paleoclimatic history of the Somali Basin during the Pliocene-Pleistocene; multivariate analyses of benthic foraminifera from DSDP Site 241(Leg 25), *J. Foraminiferal Res.*, 27(3), 196–208, doi:10.2113/gsjfr.27.3.196.

Gupta, A. K., and E. Thomas (1999), Latest Miocene-Pleistocene productivity and deep-sea ventilation in the northwestern Indian Ocean (DSDP Site 219), *Paleoceanography*, 14, 62–73, doi:10.1029/1998PA900006.

Hearty, P. J. (1998), The geology of Eleuthera Island, Bahamas: A Rosetta Stone of Quaternary stratigraphy and sea-level history, *Quat. Sci. Rev.*, 17(4–5), 333–355, doi:10.1016/S0277-3791(98)00046-8.

Hearty, P. J., P. Kindler, H. Cheng, and R. L. Edwards (1999), A +20 m middle Pleistocene sea-level highstand (Bermuda and the Bahamas) due to partial collapse of Antarctic ice, *Geology*, 27(4), 375–378, doi:10.1130/0091-7613(1999)027<0375:AMMPSL>2.3.CO;2.

Helmke, P., S. Neuer, M. W. Lomas, M. Conte, and T. Freudenthal (2010), Cross-basin differences in particulate organic carbon export and fux attenuation in the subtropical North Atlantic gyre, *Deep Sea Res., Part I*, 57, 213–227, doi:10.1016/j.dsr.2009.11.001.

Herguera, J. C. (2000), Last glacial paleoproductivity patterns in the eastern equatorial Pacific: Benthic foraminifera records, *Mar. Micropaleontol.*, *40*, 259–275, doi:10.1016/S0377-8398(00)00041-4.

Herguera, J. C., and W. H. Berger (1991), Paleoproductivity from benthic foraminifera abundance: Glacial to postglacial change in the west-equatorial Pacific, *Geology*, *19*, 1173–1176, doi:10.1130/0091-7613(1991) 019<1173:PFBFAG>2.3.CO;2.

Howard, W. R. (1997), Palaeoclimatology: A warm future in the past, *Nature*, *388*(6641), 418–419, doi:10.1038/41201.

Ishman, S. E. (1996), A benthic foraminiferal record of middle to late Pliocene (3.15–2.85 Ma) deep water change in the North Atlantic, *Mar. Micropaleontol.*, *27*, 165–180, doi:10.1016/0377-8398(95)00058-5.

Jasper, J. P., and R. B. Gagosian (1990), The sources and deposition of organic matter in the Late Quaternary Pigmy Basin, Gulf of Mexico, *Geochim. Cosmochim. Acta*, *54*, 1117–1132, doi:10.1016/0016-7037(90) 90443-O.

Jones, R. W. (1994), *The Challenger Foraminifera*, 149 pp., Oxford Univ. Press, Oxford, U. K.

Kaiho, K. (1999), Effect of organic carbon flux and dissolved oxygen on the benthic foraminiferal oxygen index (BFOI), *Mar. Micropaleontol.*, *37*, 67–76, doi:10.1016/S0377-8398(99)00008-0.

Katz, M. E., and K. G. Miller (1987), Neogene benthic foraminiferal biofacies of the New Jersey Transect, *Initial Rep. Deep Sea Drill. Proj.*, *95*, 299–311.

Keigwin, L. D., and G. A. Jones (1989), Glacial-Holocene stratigraphy, chronology and some paleoceanographic observations on some North Atlantic sediment drifts, *Deep Sea Res.*, *36*, 845–867, doi:10.1016/ 0198-0149(89)90032-0.

Keigwin, L. D., and G. A. Jones (1994), Western North Atlantic evidence for millennial-scale changes in ocean circulation and climate, *J. Geophys. Res.*, *99*(C6), 12,397–12,410, doi:10.1029/94JC00525.

Keigwin, L. D., et al. (1998), *Proceedings of the Ocean Drilling Program, Initial Reports*, vol. 172, edited by S. E. Swanson, Ocean Drill. Program, College Station, Tex.

King, S. C., J. W. Murray, and A. E. S. Kemp (1998), Palaeoenvironments of deposition of Neogene laminated diatom mat deposits from the eastern equatorial Pacific from studies of benthic foraminifera (sites 844, 849, 851), *Mar. Micropaleontol.*, *35*, 161–177, doi:10.1016/S0377-8398(98) 00020-6.

Lee, T. N., J. A. Yoder, and L. P. Atkinson (1991), Gulf Stream frontal eddy influence on productivity of the southeast U.S. Continental Shelf, *J. Geophys. Res.*, *96*(C12), 22,191–22,205, doi:10.1029/91JC02450.

Licari, L. N., S. Schumacher, F. Wenzhofer, M. Zabel, and A. Mackensen (2003), Communities and microhabitat of living benthic foraminifera from the tropical East Atlantic: Impact of different productivity regimes, *J. Foraminiferal Res.*, *33*(1), 10–31, doi:10.2113/0330010.

Lippold, J., J. Grützner, D. Winter, Y. Lahaye, A. Mangini, and M. Christl (2009), Does sedimentary ^{231}Pa/^{230}Th from the Bermuda Rise monitor past Atlantic meridional overturning circulation?, *Geophys. Res. Lett.*, *36*, L12601, doi:10.1029/2009GL038068.

Lisiecki, L. E., and M. E. Raymo (2005), A Pliocene-Pleistocene stack of 57 globally distributed benthic δ^{18}O records, *Paleoceanography*, *20*, PA1003, doi:10.1029/2004PA001071.

Loubere, P. (1991), Deep-sea benthic foraminiferal assemblage response to a surface ocean productivity gradient: A test, *Paleoceanography*, *6*(2), 193–204, doi:10.1029/90PA02612.

Loubere, P. (1996), The surface ocean productivity and bottom water oxygen signals in deep water benthic foraminifera assemblages, *Mar. Micropaleontol.*, *28*, 247–261, doi:10.1016/0377-8398(96)00004-7.

Loutre, M. F., and A. Berger (2003), Marine Isotope Stage 11 as an analogue for the present interglacial, *Global Planet. Change*, *36*(3), 209–217, doi:10.1016/S0921-8181(02)00186-8.

Lutze, G. F., and W. T. Coulbourn (1984), Recent benthic foraminifera from the continental margin of northwest Africa: Community structure and distribution, *Mar. Micropaleontol.*, *8*, 361–401, doi:10.1016/0377-8398(84)90002-1.

Mackensen, A., H. P. Sejrup, and E. Jansen (1985), The distribution of living benthic foraminifera on the continental slope and rise off southwest Norway, *Mar. Micropaleontol.*, *9*(4), 275–306, doi:10.1016/0377-8398(85) 90001-5.

Mackensen, A., D. K. Futterer, H. Grobe, and G. Schmiedl (1993), Benthic foraminifera assemblages from eastern South Atlantic Polar Front region between 35° and 57°S: Distribution, ecology and fossilization potential, *Mar. Micropaleontol.*, *22*, 33–69, doi:10.1016/0377-8398(93)90003-G.

Mackensen, A., G. Schmiedl, J. Harloff, and M. Giese (1995), Deep-sea foraminifera in the South Atlantic Ocean: Ecology and assemblage generation, *Micropaleontology*, *41*(4), 342–358, doi:10.2307/1485808.

McClain, C. R., S. R. Signorini, and J. R. Christian (2004), Subtropical gyre variability observed by ocean-color satellites, *Deep Sea Res., Part II*, *51*(1–3), 281–301, doi:10.1016/j.dsr2.2003.08.002.

McManus, J., D. Oppo, J. Cullen, and S. Healey (2003), Marine Isotope Stage 11 (MIS 11): Analog for Holocene and future climate?, in *Earth's Climate and Orbital Eccentricity: The Marine Isotope Stage 11 Question*, *Geophys. Monogr. Ser.*, vol. 137, edited by A. W. Droxler, R. Z. Poore, and L. H. Burckle, pp. 69–85, AGU, Washington, D. C., doi:10.1029/ 137GM06.

McManus, J. F., S. Drown-Leger, R. Francois, J. M. Gherardl, and L. Kelgwin (2004), Collapse and rapid resumption of Atlantic meridional circulation linked to deglacial climate changes, *Nature*, *428*(6985), 834–837, doi:10.1038/nature02494.

Meyers, P. A. (1994), Preservation of elemental and isotopic source identification of sedimentary organic matter, *Chem. Geol.*, *114*, 289–302, doi:10.1016/0009-2541(94)90059-0.

Miao, Q., and R. C. Thunell (1993), Recent deep-sea benthic foraminiferal distributions in the South China and Sulu Seas, *Mar. Micropaleontol.*, *22*(1–2), 1–32, doi:10.1016/0377-8398(93)90002-F.

Mix, A. C. (1989), Influence of productivity variations on long-term atmospheric CO_2, *Nature*, *337*, 541–544, doi:10.1038/337541a0.

Morigi, C., F. J. Jorissen, A. Gervais, S. Guichard, and A. M. Borsetti (2001), Benthic foraminiferal faunas in surface sediments off NW Africa: Relationship with organic flux to the ocean floor, *J. Foraminiferal Res.*, *31*(4), 350–368, doi:10.2113/0310350.

Murgese, D. S., and P. De Deckker (2005), The distribution of deep-sea benthic foraminifera in core tops from the eastern Indian Ocean, *Mar. Micropaleontol.*, *56*(1–2), 25–49, doi:10.1016/j.marmicro.2005.03.005.

Nave, S., L. Labeyrie, J. M. Gherardl, N. Caillon, E. Cortijo, C. Kissel, and F. Abrantes (2007), Primary productivity response to Heinrich events in the North Atlantic Ocean and Norwegian Sea, *Paleoceanography*, *22*, PA3216, doi:10.1029/2006PA001335.

Nees, S., A. V. Altenbach, H. Kassens, and J. Thiede (1997), High-resolution record of foraminiferal response to late Quaternary sea-ice retreat in the Norwegian-Greenland Sea, *Geology*, *25*(7), 659–662, doi:10.1130/0091-7613(1997)025<0659:HRROFR>2.3.CO;2.

Ohkouchi, N., T. I. Eglinton, L. D. Keigwin, and J. M. Hayes (2002), Spatial and temporal offsets between proxy records in a sediment drift, *Science*, *298*(5596), 1224–1227, doi:10.1126/science.1075287.

Ohkushi, K., E. Thomas, and H. Kawahata (1999), Abyssal benthic foraminifera from the Northwestern Pacific (Shatsky Rise) during the last 298 kyr, *Mar. Micropaleontol.*, *38*(2), 119–147, doi:10.1016/S0377-8398(99)00040-7.

Olson, S. L., and P. J. Hearty (2009), A sustained +21 m sea-level highstand during MIS 11(400 ka): Direct fossil and sedimentary evidence from Bermuda, *Quat. Sci. Rev.*, *28*(3–4), 271–285, doi:10.1016/j.quascirev. 2008.11.001.

Pflaumann, U., et al. (2003), Glacial North Atlantic: Sea-surface conditions reconstructed by GLAMAP 2000, *Paleoceanography*, *18*(3), 1065, doi:10.1029/2002PA000774.

Poli, M. S., R. C. Thunell, and D. Rio (2000), Millennial-scale changes in North Atlantic Deep Water circulation during marine isotope stages 11 and 12: Linkage to Antarctic climate, *Geology*, *28*(9), 807–810, doi:10.1130/0091-7613(2000)28<807:MCINAD>2.0.CO;2.

Poli, M. S., P. A. Meyers, and R. C. Thunell (2010), The western North Atlantic record of MIS 13 to 10: Changes in primary productivity, organic carbon accumulation and benthic foraminiferal assemblages in sediments from the Blake Outer Ridge (ODP Site 1058), *Palaeogeogr. Palaeoclimatol. Palaeoecol.*, *295*(1–2), 89–101, doi:10.1016/j.palaeo. 2010.05.018.

Polovina, J. J., E. A. Howell, and M. Abecassis (2008), Ocean's least productive waters are expanding, *Geophys. Res. Lett.*, *35*, L03618, doi:10.1029/2007GL031745.

Prahl, F. G., G. J. de Lange, S. Scholten, and G. L. Cowie (1997), A case of post-depositional aerobic degradation of terrestrial organic matter in turbidite deposits from the Madeira Abyssal Plain, *Org. Geochem.*, *27*, 141–152, doi:10.1016/S0146-6380(97)00078-8.

Radi, T., and A. de Vernal (2008), Last glacial maximum (LGM) primary productivity in the northern North Atlantic Ocean, *Can. J. Earth Sci.*, *45*, 1299–1316, doi:10.1139/E08-059.

Rasmussen, T. L., E. Thomsen, T. C. E. Van Weering, and L. Labeyrie (1996), Rapid changes in surface and deep water conditions at the Fareoe Margin during the last 58,000 years, *Paleoceanography*, *11*(6), 757–771, doi:10.1029/96PA02618.

Rasmussen, T. L., D. Bäckström, J. Heinemeier, D. Klitgaard-Kristensen, P. C. Knutz, A. Kuijpers, S. Lassen, E. Thomsen, S. R. Troelstra, and T. C. E. Van Weering (2002), The Faroe-Shetland gateway: Late

Quaternary water mass exchange between the Nordic seas and the north-eastern Atlantic, *Mar. Geol.*, *188*, 165–192, doi:10.1016/S0025-3227(02)00280-3.

Rasmussen, T. L., D. W. Oppo, E. Thomsen, and S. J. Lehman (2003), Deep sea records from the southeast Labrador Sea: Ocean circulation changes and ice-rafting events during the last 160,000 years, *Paleoceanography*, *18*(1), 1018, doi:10.1029/2001PA000736.

Rathburn, A. E., and B. H. Corliss (1994), The ecology of living (stained) deep-sea benthic foraminifera from the Sulu Sea, *Paleoceanography*, *9*(1), 87–150, doi:10.1029/93PA02327.

Raymo, M. E., W. F. Ruddiman, N. J. Shackleton, and D. W. Oppo (1990), Evolution of Atlantic-Pacific δ^{13}C gradients over the last 2.5 m.y, *Earth Planet. Sci. Lett.*, *97*, 353–368, doi:10.1016/0012-821X(90)90051-X.

Rohling, E. J., M. Fenton, F. J. Jorissen, P. Bertrand, G. Ganssen, and J. P. Caulet (1998), Magnitudes of sea-level lowstands of the past 500,000 years, *Nature*, *394*, 162–165, doi:10.1038/28134.

Ruddiman, W. F. (2005), Cold climate during the closest Stage 11 analog to recent millennia, *Quat. Sci. Rev.*, *24*(10–11), 1111–1121, doi:10.1016/j.quascirev.2004.10.012.

Sancetta, C. (1992), Primary production in the glacial North Atlantic and North Pacific oceans, *Nature*, *360*(6401), 249–251, doi:10.1038/360249a0.

Sarmiento, J. L., G. Thiele, R. M. Key, and W. S. Moore (1990), Oxygen and nitrate new production and remineralization in the North Atlantic Subtropical Gyre, *J. Geophys. Res.*, *95*(C10), 18,303–18,315, doi:10.1029/JC095iC10p18303.

Sarmiento, J. L., T. M. C. Hughes, R. J. Stouffer, and S. Manabe (1998), Simulated response of the ocean carbon cycle to anthropogenic climate warming, *Nature*, *393*, 245–249, doi:10.1038/30455.

Sarmiento, J. L., et al. (2004), Response of ocean ecosystems to climate warming, *Global Biogeochem. Cycles*, *18*, GB3003, doi:10.1029/2003GB002134.

Schmiedl, G., and A. Mackensen (1997), Late quaternary paleoproductivity and deep water circulation in the eastern South Atlantic Ocean: Evidence from benthic foraminifera, *Palaeogeogr. Palaeoclimatol. Palaeoecol.*, *130*(1–4), 43–80, doi:10.1016/S0031-0182(96)00137-X.

Schmittner, A. (2005), Decline of the marine ecosystem caused by a reduction in the Atlantic overturning circulation, *Nature*, *434*, 628–633, doi:10.1038/nature03476.

Schmittner, A., A. Oschlies, H. D. Matthews, and E. D. Galbraith (2008), Future changes in climate, ocean circulation, ecosystems, and bio-geochemical cycling simulated for a business-as-usual CO_2 emission scenario until year 4000 AD, *Global Biogeochem. Cycles*, *22*, GB1013, doi:10.1029/2007GB002953.

Schnitker, D. (1974), West Atlantic abyssal circulation during the past 120,000 years, *Nature*, *248*, 385–387, doi:10.1038/248385a0.

Schnitker, D. (1979), The deep waters of the western North Atlantic during the past 24,000 years, and the re-initiation of the Western Boundary Undercurrent, *Mar. Micropaleontol.*, *4*, 265–280, doi:10.1016/0377-8398(79)90020-3.

Schnitker, D. (1980), Quaternary deep-sea benthic foraminifers and bottom water masses, *Annu. Rev. Earth Planet. Sci.*, *8*, 343–370, doi:10.1146/annurev.ea.08.050180.002015.

Schwarz, J. N., and M. P. Schodlok (2009), Impact of drifting icebergs on surface phytoplankton biomass in the Southern Ocean: Ocean colour remote sensing and in situ iceberg tracking, *Deep Sea Res., Part I*, *56*, 1727–1741, doi:10.1016/j.dsr.2009.05.003.

Shackleton, N. J., M. A. Hall, J. Line, and C. Shuxi (1983), Carbon isotope data in core V19–30 confirm reduced carbon dioxide concentration in the ice age atmosphere, *Nature*, *306*(5941), 319–322, doi:10.1038/306319a0.

Smart, C. W. (2008), Abyssal NE Atlantic benthic foraminifera during the last 15 kyr: Relation to variations in seasonality of productivity, *Mar. Micropaleontol.*, *69*, 193–211, doi:10.1016/j.marmicro.2008.07.007.

Smart, C. W., and A. J. Gooday (1997), Recent benthic foraminifera in the abyssal northeast Atlantic Ocean: Relation to phytodetrital inputs, *J. Foraminiferal Res.*, *27*(2), 85–92, doi:10.2113/gsjfr.27.2.85.

Smart, C. W., S. C. King, A. J. Gooday, J. W. Murray, and E. Thomas (1994), A benthic foraminiferal proxy of pulsed organic matter paleo-fluxes, *Mar. Micropaleontol.*, *23*, 89–99, doi:10.1016/0377-8398(94)90002-7.

Smart, C. W., C. Waelbroeck, E. Michel, and A. Mazaud (2010), Benthic foraminiferal abundance and stable isotope changes in the Indian Ocean sector of the Southern Ocean during the last 20 kyr: Paleoceanographic implications, *Palaeogeogr. Palaeoclimatol. Palaeoecol.*, *297*, 537–548, doi:10.1016/j.palaeo.2010.08.011.

Smith, K., B. H. Robison, J. J. Helly, R. S. Kaufmann, H. A. Ruhl, T. J. Shaw, B. S. Twining, and M. Vernet (2007), Free-drifting icebergs: Hot spots of chemical and biological enrichment in the Weddell Sea, *Science*, *317*, 478–482, doi:10.1126/science.1142834.

Stein, R., J. Hefter, J. Grutzner, A. Voelker, and B. D. A. Naafs (2009), Variability of surface water characteristics and Heinrich-like events in the Pleistocene midlatitude North Atlantic Ocean: Biomarker and XRD records from IODP Site U1313(MIS 16–9), *Paleoceanography*, *24*, PA2203, doi:10.1029/2008PA001639.

Steinacher, M., et al. (2010), Projected 21st century decrease in marine productivity: A multi-model analysis, *Biogeosciences*, *7*(3), 979–1005, doi:10.5194/bg-7-979-2010.

Suess, E., and P. J. Müller (1980), Productivity, sedimentation rate and sed-imentary organic matter in the oceans II.- Elemental fractionation, *Colloq. Int. C. N. R. S.*, *293*, 17–26.

Sun, X., B. H. Corliss, C. W. Brown, and W. J. Showers (2006), The effect of primary productivity and seasonality on the distribution of deep-sea benthic foraminifera in the North Atlantic, *Deep Sea Res., Part I*, *53*, 28–47, doi:10.1016/j.dsr.2005.07.003.

Thierstein, H. R., B. Molfino, K. Geitzenauer, and N. J. Shackleton (1977), Global synchroneity of late Quaternary coccolith datum levels; validation by oxygen isotopes, *Geology*, *5*, 400–404, doi:10.1130/0091-7613(1977)5<400:GSOLQC>2.0.CO;2.

Thomas, E., and A. J. Gooday (1996), Cenozoic deep-sea benthic fora-minifers: Tracers for changes in oceanic productivity?, *Geology*, *24*(4), 355–358, doi:10.1130/0091-7613(1996)024<0355:CDSBFT>2.3.CO;2.

Thomas, E., L. Booth, M. Maslin, and N. Shackleton (1995), Northeastern Atlantic benthic foraminifera during the last 45,000 years: Changes in productivity seen from the bottom up, *Paleoceanography*, *10*(3), 545–562, doi:10.1029/94PA03056.

Verardo, D. J., and A. McIntyre (1994), Production and destruction: Con-trol of biogenous sedimentation in the tropical Atlantic 0–300 000 years BP, *Paleoceanography*, *9*, 63–86, doi:10.1029/93PA02901.

Villanueva, J., E. Calvo, C. Pelejero, J. O. Grimalt, A. Boelaert, and L. D. Labeyrie (2001), A latitudinal productivity band in the central North Atlantic over the past 20 kyr: An alkenone perspective, *Paleoceanogra-phy*, *16*, 617–626, doi:10.1029/2000PA000543.

Yoder, J. A., L. P. Atkinson, T. N. Lee, H. H. Kim, and C. R. McClain (1981), Role of the Gulf Stream frontal eddies in forming phyto-plankton patches on the outer southeastern shelf, *Limnol. Oceanogr.*, *26*, 1103–1110, doi:10.4319/lo.1981.26.6.1103.

Yoder, J. A., S. G. Ackleson, R. T. Barber, P. Flament, and W. M. Balch (1994), A line in the sea, *Nature*, *371*, 689–692, doi:10.1038/371689a0.